

JAN. - APR. 2004
Volume X Number I

ISSN 0859 144X

THE ASEAN JOURNAL OF RADIOLOGY

Published by The Radiological Society and
The Royal College of Radiologists of Thailand,
Bangkok, Thailand

Started through an educational grant from Bracco since 1995



THE IMAGE OF INNOVATION

JAN. - APR. 2004

Volume X Number I

ISSN 0859 144X

THE ASEAN JOURNAL OF RADIOLOGY

Published by The Radiological Society and
The Royal College of Radiologists of Thailand,
Bangkok, Thailand

Started through an educational grant from Bracco since 1995



www.bracco.com

THE IMAGE OF INNOVATION

Chief Editor

Professor Kawee Tungsubutra
Kaweevej Hospital, 318 Taksin Road, Dhonburi, Bangkok 10600, Thailand.

Asean Journal of Radiology.
Instructions for Authors.

1. The Asean Journal of Radiology publishes the papers on Radiological Sciences, such as research work, review articles, case reports, innovations in Medical Sciences related to all branches of Radiology, and letters to the editor. The aforementioned materials can be written in English only.

2. The authors have to submit 2 copies of the manuscript and a diskette: **to Prof. Dr. Kawee Tungsubuttra**, 318 Kaweevej Hospital, Taksin Road, Dhonburi, Bangkok 10600, Thailand.

3. The original copy to be submitted must be typed in a double space on one side of the page of 8.1/2" x 11.1/2" paper.

4. The format of the article must include :

- a. Title page and address of the author (s)
- b. Abstract
- c. Introduction (Background)
- d. Material and Method
- e. Results and discussion (Tables and Illustrations)
- f. Acknowledgement (if any)
- g. References (Follow the Vancouver style developed by ICMJE)

5. We will provide 5 copies of reprints for the author (s) who submit (s) an article for publication in the Asean Journal.

6. The illustrations and tables must be clearly prepared with legends in English as they are the art works to be reproduced.

7. The authors are responsible for the contents of the article as to its facts and findings.

8. Ethics.

Paper reporting studies which might be interpreted as human experimentation (e.g. controlled trials) should conform to the standards of the Declaration of Helsinki (see British Medical Journal 1964;2:177) and should indicate that, approval that such studies may proceed, has been granted by the local or hospital Ethics Committee.

When reporting experiments on animals indicate whether the institution's or the National Research Council's guide for, or any national law on, the care and use of laboratory animals was followed.

THE ASEAN JOURNAL OF RADIOLOGY

Editor-in-Chief

Professor Kawee Tungsubutra
Kaweevej Hospital, 318 Tarksin Road, Dhonburi, Bangkok 10600, Thailand.

Associate Editors.

Wilaiporn Bhotisuwan, M.D. Sutthisak Sutthipongchai, M.D.
Walaya Wongsivatchai, M.D.

Emeritus Editors

Saroj Vanapruks, M.D.
Chorfa Kaewjinda, M.D.
Sutee Na Songkhla, M.D.
Poonsook Jitnusun, M.D.

EDITORIAL BOARD :

Body Computed Tomography	Linda Brown, M.D.
Breast Imaging	Chutakiat Krautachue, M.D.
Gastrointestinal Imaging	Wilaiporn Bhotisuwan, M.D.
Genitourinary Imaging	Darunee Boonyuenvetwat, M.D.
Head and Neck Imaging	Narumol Srisuthapan Hargrove, M.D.
Magnetic Resonance Imaging	Panruethai Trinavarat, M.D.
Musculoskeletal Imaging	Walaya Wongsivatchai, M.D.
Neuroradiology	Walailak Chaiyasoot, M.D.
Nuclear Medicine	Jiraporn Laothamatas, M.D.
Pediatric Imaging	Somchai Panyasungkha, M.D.
Radiation Oncology	Krisdee Prabhasawat, M.D.
Thoracic Imaging	Napawadee Impoolsup, M.D.
Ultrasonography	Supaneewan Jaovasidha, M.D.
Vascular Interventional Radiology	Nittaya Lektrakul, M.D.
Treasurer	Sirintara Pongpetch, M.D.
	Orasa Chawarnparit, M.D.
	Vacharin Ratanamart, M.D.
	Pawana Pusuwan, M.D.
	Tawatchai Chaaiwatanarat, M.D.
	Sriprapai Kaewrojana, M.D.
	Anchalee Kruatrachue, M.D.
	Pittayapoom Pattaranutaporn, M.D.
	Pramook Phromratanapongse, M.D.
	Yongyut Kongthanasat, M.D.
	Supranee Nirapathpongsporn, M.D.
	Ponglada Subhannachart, M.D.
	Laddawan Vajragupta, M.D.
	Srinart Sangsa-Ard, M.D.
	Chamaree Chuapetcharasopon, M.D.
	Anchalee Churojana, M.D.
	Nopporn Beokhaimook, M.D.

CONTENTS

	Page
1. ADRENAL VASCULAR (ENDOTHELIAL) CYST: A CASE REPORT AND LITERATURE REVIEW Wattanawan EUAPITAKSAKUL, Surasuk TAWIPORNCHAI, Benjaporn CHAIWUN	1-6
2. THE ROLE OF SONOGRAPHY IN THE DIAGNOSIS OF TRAUMATIC RUPTURE OF THE ANTERIOR CRUCIATE LIGAMENT OF THE KNEE Piyadara KHONGPIBOONKIT, Chairat KHONGPIBOONKIT, Worachai AUEAPINUN, Anun MALAIRUNGSAKUL	7-14
3. INTER-COMPARISON OF ACQUISITION AND PROCESSING SOFTWARE FOR MUGA STUDY AND PIP Chatchai NAVIKHACHEEVIN	15-24
4. LARGE PAPILLARY CARCINOMA OF URINARY BLADDER Siriporn POOLSIRI, Chakrit HEKPHEERA	25-30
5. HEMOPTYSIS CAUSED BY A MIGRATORY K-WIRE: A CASE REPORT AND REVIEW LITERATURE Nitaya THONGSIBKAO	31-34
6. THE STUDY OF ABSORBED DOSE DETERMINATION IN HIGH ENERGY ELECTRON AND PHOTON BEAMS USING NEW CODE OF PRACTICE IAEA-TRS 398 COMPARED WITH IAEA-TRS 277 Sivalee SURIYAPEE, Tassanee LAYANGKUL, Surat VINIJSORN, Siri SRIMANOROTH	35-40
7. GASTRIC OUTLET OBSTRUCTION DURING BONE SCAN Dr. M.A. Taher	41-43
8. NUCLEAR ONCOLOGY Dr. M.A. Taher	45-48
9. MATERNAL SCREENING OF THYROID FUNCTION Dr. M.A. Taher	49-50

THE ASEAN JOURNAL OF RADIOLOGY

Volume X Number I JAN. - APR. 2004

CONTENTS

	Page
10. URETEROPELVIC JUNCTION OBSTRUCTION (UPJO) PRESENTED AS HEMATURIA. Dr. M.A. Taher	51-52
11. ULTRASOUND IN CHRONIC ECTOPIC PREGNANCY Dr. M.A. Taher	53-54
12. CASE REPORT: TRAUMATIC LACERATION OF LIVER AND HAEMOPERITONIUM. Dr. Md. Murshed Ali, Dr. S.M.A Taleb	55-56
13. CASE REPORT Dr. Md. Murshed Ali, Dr. JaharAtul ferdous	57-59
14. FETAL ULTRASOUND BIOMETRY Dr. M.A. Taher	61-63
15. SONOGRAPHIC MEASUREMENT OF RENAL SIZE IN NORMAL BANGLADESHI CHILDREN Ashoke Kumar PAUL, Choudhury Habibur RASULX, Hosne Ara RAHMAN, Sayedur Rahman MIAH	65-68
16. UNEQUAL TWIN: CASE REPORT Dr. M.A. Taher	69-70
17. FUTURE OF EMERGENCY ULTRASOUND Dr. M.A.Taher	71-74

ADRENAL VASCULAR (ENDOTHELIAL) CYST: A CASE REPORT AND LITERATURE REVIEW

Wattanawan EUAPITAKSAKUL¹, Surasuk TAWIPORNCHAI²,
Benjaporn CHAIWUN³

ABSTRACT

Adrenal vascular (endothelial) cysts are rare adrenal lesions. Herein, we reported a case of adrenal endothelial cyst in a 30-year-old pregnant woman. The patient had a 10-day history of left upper quadrant pain. Abdominal ultrasonography and computed tomography showed a huge hemorrhagic cystic lesion superior to the left kidney. Calcified cyst wall with internal septae was also noted. The microscopic examinations revealed multiloculated cysts lined focally by benign flattened endothelial cells. The general feature, differential diagnosis, pathogenesis, and management of adrenal cysts were discussed.

INTRODUCTION

Adrenal vascular (endothelial) cysts are rare.¹ They vary greatly in size from microscopic to more than 50 cm in diameter. Symptoms, particularly in large cysts, are usually associated with compression effect to surrounding visceral organs, leading to pain and vague abdominal symptoms. On the contrary, smaller ones are incidentally found during the evaluation of unrelated abdominal conditions. Clinically, the differential diagnosis of adrenal vascular cysts is diverse, including any lesion that can present with upper abdominal mass for instance, adrenal neoplasms, hepatic cysts and hemangiomas, polycystic kidneys, hydronephrosis, cystic renal cortical adenomas and carcinomas, Wilms' tumor, pancreatic, mesenteric and urachal cysts, and retroperitoneal tumors. Our aim was to report a rare case of adrenal vascular cyst recognized by ultrasonography and computed tomography.

CASE REPORT

Clinical information:

A 30-year-old woman with 15-week gestation pregnancy presented to the gynecological service with a 10 days history of left upper quadrant pain. Physical examination revealed a positive left kidney's punch. The basic laboratories were normal. The abdominal ultrasonography (US) showed a well-defined 10x15 cm thin wall cystic mass with hemorrhagic content over the left suprarenal region (figure 1). The left kidney was displaced downward to the left lower quadrant of the abdomen. Both kidneys were grossly unremarkable. The computed tomography (CT) revealed a huge 10x13x15 cm hemorrhagic cystic mass at the left suprarenal region with enhanced internal septae after contrast administration (figure 2). According to the findings, a provisional diagnosis was hemorrhagic adrenal cyst.

¹ Department of Radiology,

² Department of Surgery, Phayao Hospital, Meung, Phayao, 56000 Thailand

³ Department of Pathology, Faculty of medicine, Chiang Mai University, Thailand

Running title: Adrenal endothelial cyst

Keywords: Adrenal mass, diagnosis, ultrasound, computed tomography, pathology

Corresponding author: Wattanawan Euapitaksakul, M.D. Department of Radiology, Phayao Hospital Amphur Meung, Phayao 56000 THAILAND



Fig. 1 Ultrasonography shows a well-defined thin wall cystic mass (arrow) with hyperechoic content. A small calcification at cyst wall is also shown.

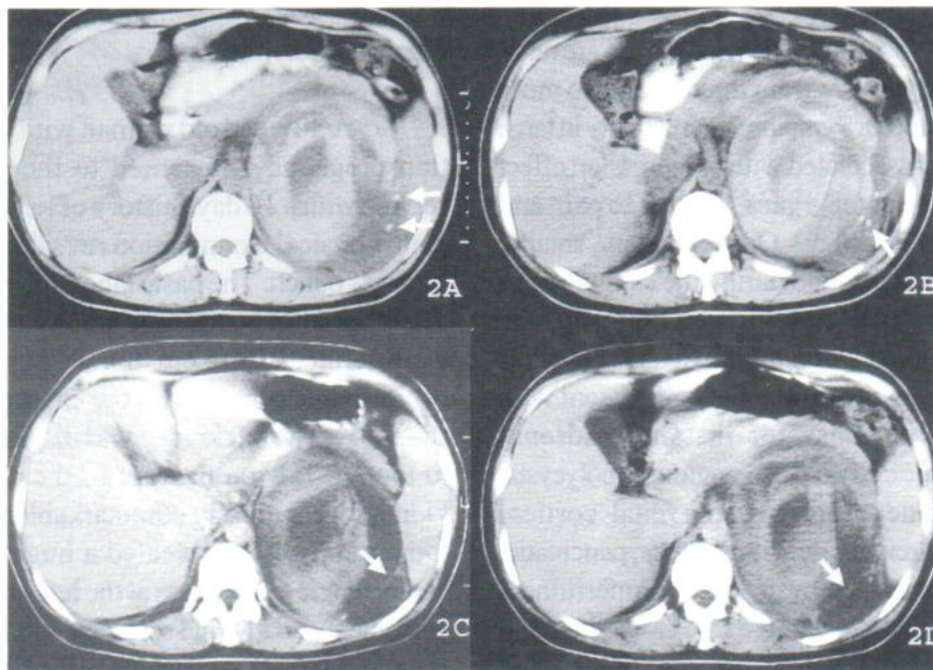


Fig. 2 (A and B) Non-enhanced CT scan through left suprarenal region shows a large heterogeneous mass at the left suprarenal region with anterior displacement of the pancreas. The high attenuation areas consistent with hemorrhage. Calcifications in the wall of the mass (arrows) are shown. (C and D) Contrast-enhanced CT scan shows a well-delineated internal septae.

Because the cyst was larger than 5 cm in diameter, an exploratory laparotomy was performed. Intraoperatively, a huge transparently thin wall cyst filled with 1300 ml of hemorrhagic fluid was found in the left retroperitoneal space. Since, the inferior margin could not be separated from the left kidney, the cyst and the left kidney were removed (figure3).

The histopathologic study revealed multiloculated cysts focally lined by benign flattened endothelial cells. The cyst contents consisted of bloody materials. The intervening stroma focally revealed benign adrenal tissue as well as focal hemorrhage. No definite malignancy was observed (figure 4).



Fig. 3 Gross pathology of adrenal cyst is shown.

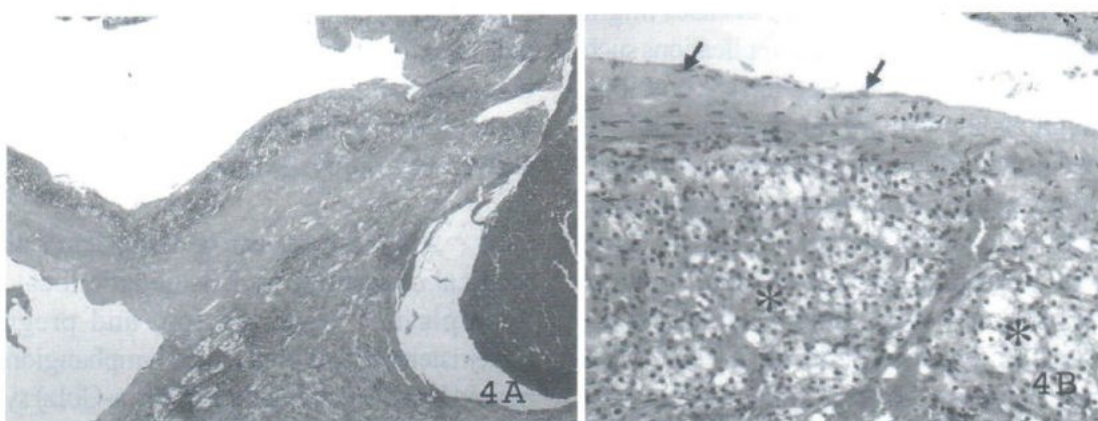


Fig. 4 Microscopic sections show multiloculated cysts (H&Ex40) (A) lined by benign endothelial cells (arrow) with sheets of benign adrenal cortical cells in the stroma (astrix) (H&Ex200) (B)

DISCUSSION

Adrenal cysts are rare tumefactive lesions, with the reported incidence of 0.06-0.18%.² They can occur at any age, but are more commonly seen in the fifth and sixth decades of life.¹ Less than five percent of the cases occur in children.³ Females are more affected than males. The adrenal cyst is often noted unilaterally, in which it is more commonly seen on the right side; only 5-8% is bilateral. Symptoms and signs are usually nonspecific, such as dull flank pain, epigastric distress or indigestion, and a palpable abdominal mass.⁴ Occasionally, these might accompany with constitutional symptoms, for example malaise and weakness. Fever with leukocytosis is rare. Intracystic hemorrhage can result in anemia and a slowly growing abdominal mass.¹

Adrenal cysts have been classified into four major types, including endothelial cyst, pseudocyst, epithelial-lined or true adrenal cyst, and parasitic cysts.¹ Among those, the endothelial cysts are the most common reported (45%), in which they typically originate from lymphatic vessels, called lymphagimatus cysts (41%). However, some can rarely derived from capillaries, named angiomatous cysts. Adrenal endothelial cysts are usually incidentally found, but in exceptional cases might present with hypertension.⁵ Acute complications such as hemorrhage, rupture, and infection are possible. Plain radiographs show mural calcifications in 15% of the cases.⁶ Although the cyst wall is thin and smooth containing homogenous liquid contents, it, sometimes, shows slightly echoic or hyperechoic at imaging. Large cysts need to be distinguished from renal, hepatic, splenic and pancreatic cysts. Multiplanar images are helpful in localizing the origin of the cyst. The pseudocysts (39%) are the most common clinically recognized type of adrenal cyst encountered during surgery.⁷ It is usually large and develops in elderly patients. However, a recent report showed giant adrenal cysts occurring in three teenage girls.⁸ The walls are composed of dense fibrous connective tissue with islands of adrenal cortical tissue incorpo-

rated. Bleeding into the normal adrenal gland or tumor might be responsible for the formation of pseudocysts. This postulation is supported by a report of children having pseudocyst following adrenal hemorrhage as a result of injury or infarction in the neonatal period.⁹ If the cyst is lined by epithelial, it is called true cyst, occurring in 9% of the cases. They can subdivided into true glandular or retention cysts, embryonal cysts and cystic degeneration of adrenal tumors.¹⁰ Most of the malignant adrenal cysts are metastatic (95%), followed by pheochromocytoma (3%) and adrenocortical carcinoma (2%).¹¹ Malignancy should be suspected if the patients present with hormonal disturbances and hypertension. A retrospective review of the ultrasonographic feature of adrenal lesions revealed that focal absence of periglandular fat between the adrenal gland and the large vessels or liver, as well as deviation or compression of the large vessels by the adrenal lesion, may indicate malignancy.¹² Although calcification could be seen in either benign or malignant lesion, a thickened and irregular cyst wall should be suspected of malignancy. Finally, the parasitic cyst (7%) usually occurs after disseminated *Echinococcus granulosus* infection.¹³ The content is initially purely liquid and is limited by two layers. The inner (germinal) layer is composed of the parasite, whereas the outer layer allows the passage of nutrients. The inner layer produces the laminar membrane and scoleces and secretes the cystic fluid.

Adrenal cysts can be associated with certain medical conditions such as hepatic focal nodular hyperplasia,¹⁴ hypertension, and pregnancy.¹⁵ Co-existence of adrenal cystic lymphangiomas with nevroid basal cell carcinoma (Gorlin-Golz) syndrome were reported.¹⁶

Radiological differential diagnosis of adrenal cysts should include cystic lesions in the adjacent organs such as the liver, spleen, kidneys, and cystic retroperitoneal tumors as well as other rare congeni-

tal abnormalities, such as bronchogenic cysts.¹⁷

Hemorrhage in adrenal gland occurs secondarily to both traumatic and nontraumatic conditions. Nontraumatic adrenal hemorrhage, however, is uncommon and may be associated with a variety of conditions including sepsis, burn, hypotension, pregnancy, cardiovascular disease, exogenous steroid, bleeding diathesis, and underlying adrenal tumors.¹⁸ Stress events, as mentioned previously, stimulate endogenous secretion of adrenocorticotrophic hormone, resulting in a marked increase in adrenal vascularity and subsequently intraglandular hemorrhage. The lesion is more commonly seen on the right side, in which this could be attributed to compression of the adrenal gland between the liver and kidney.¹⁹ A primary adrenal cyst or tumor was reported to be the fourth most common causes of spontaneous retroperitoneal hemorrhage after renal cell carcinoma, angiomyolipoma, and renal artery aneurysm.²⁰ Although a cortical adenoma is the most common neoplasm of the adrenal gland, massive hemorrhage from an adenoma is extremely rare, probably due to its hypovascular nature.^{21,22} Pheochromocytoma is the most common cause of massive bleeding from a primary adrenal tumor, whereas bronchogenic carcinoma is the most common cause of hemorrhagic adrenal metastases.¹⁹

Unfortunately, clinical and imaging findings alone and even fine-needle aspiration, cannot always make the diagnosis and differential diagnoses of these lesions. Surgical biopsy is always needed. Ultrasound, CT, and MRI have been reported having diagnostic sensitivities of 66.7%, 80%, and 100%, respectively.²³

Management of adrenal cysts depends on clinical and imaging findings and diagnosis. Surgical excision, when possible by laparoscopic approach, is indicated in the presence of symptoms, endocrine abnormalities (even when subclinical), complications, and suspicion of malignancy. In a small cyst without evidence of malignancy, the patient may be treated

conservatively with regular follow-up by ultrasonography or CT and hormonal evaluation.

In summary, a case of adrenal vascular (endothelial) cyst, a rare entity, is reported here with its radiological and pathological findings. The diagnosis of different types of adrenal cystic lesions and their differentiation from cystic lesions of adjacent organs are critical for clinical management. The combination of clinical, laboratory, and imaging findings is essential. It is important for the radiologist to be familiar with the characteristic appearance of different cystic adrenal lesions in order to guide diagnosis and patient management.

REFERENCES

1. Abeshouse GA, Goldstein RB, Abeshouse BS. Adrenal cysts: review of the literature and report of three cases. *J Urol* 1959;81:711-9.
2. Wahi HR. Adrenal cysts. *Am J Pathol* 1951;27: 758-61.
3. Barron SH, Emanuel B. Adrenal cyst: a case report and review of pediatric literature. *J Pediatr* 1961;59:592-9.
4. Travis WD, Oertel JE, Lack EE. Miscellaneous tumors and tumefactive lesions of the adrenal gland. In: Lake EE, editor. *Pathology of adrenal glands*. New York: Churchill Livingstone, 1990:p.351-78.
5. Gigas JM, Bucy JG, Truxler G, et al. Cystic hamartoma of the adrenal gland associated with hypertension. *J Urol* 1972;107:161-2.
6. Scheible W, Coel M, Siemers PT, Seigle H. Percutaneous aspiration of adrenal cysts. *AJR* 1977;128:1013-6.
7. Foster D. Adrenal cysts: review of literature and report of case. *Arch Surg* 1966; 92: 131-43.
8. Broadley P, Daneman A, Wesson D, et. al. Large adrenal cysts in teenage girls: diagnostic and management. *Pediatr Radiol*. 1997; 27:550-2.

9. Zivkovic SM, Jancie-Z guricas M, Jukanovic R. Adrenal cysts in newborn J Urol 1983; 129:1031-3.
10. Kearney GP, Mahoney EM, Maher E, Harrison JH. Functioning and nonfunctioning cysts of the adrenal cortex and medulla. Am J Surg 1977;134:363-8.
11. Outwater E, Bankoff MS. Clinically significant adrenal hemorrhages secondary to metastases: computed tomographic observations. Clin Image 1989;13:195-200.
12. Besso JG, Tidwell AS, Gliatto JM. Retrospective review of the ultrasonographic features of adrenal lesions in 21 ferrets. Vet Radiol Ultrasound 2000;41:345-52.
13. Otal P, Escourrou G, Mazerolles C, et al. Imaging features of uncommon adrenal masses with histopathologic correlation. Radiographics 1999;19:569-81.
14. Chetty R, Dada MA. Focal nodular hyperplasia of the liver coexisting with an adrenal pseudocyst. S Afr J Surg 1998;36:82-3.
15. Uretzky G, Freund H, Charuzi, Iutwak EM. Cysts of the adrenal gland. Eur Urol 1978; 4:97-9.
16. Morteale KJ, Hoier MR, Mergo PJ, Ros PR. Bilateral adrenal cystic lymphangiomas in nevoid basal cell carcinoma (Gorlin-Golz) syndrome: US, CT, and MR findings. J Comput Assist Tomogr. 1999;23:562-4.
17. Reichelt O, Grieser T, Wunderlich H, et al. Bronchogenic cyst: a rare differential diagnosis of retroperitoneal tumors. Urol Int. 2000; 64:216-9.
18. Rao RH, Vagnucci AH, Amico JA. Bilateral massive adrenal hemorrhage: early recognition and treatment. Ann Intern Med 1989; 110:227-35.
19. Akira K, Carl MS, Randy DE, et al. Imaging of nontraumatic hemorrhagic of the adrenal gland. RadioGraphics 1999;19:949-63.
20. Swift DL, Lingeman JE, Baum WC. Spontaneous retroperitoneal hemorrhage: a diagnosis challenge. J Urol 1980;123:577-82.
21. De Resende Alves JB, de Alvarenga RJ, Kingma J, Meyer TN. Adenoma and hemorrhage of the adrenal gland. Int Surg 1976; 61:429-30.
22. Anderson WM, Timberline GA. Massive retroperitoneal hemorrhage from an asymptomatic adrenal cortical adenoma. Am Surg 1989;5:299-302.
23. Bellantone R, Ferrante A, Raffaelli M, et al. Adrenal cystic lesions: report of 12 surgically treated cases and review of literature. J Endocrinol Invest 1998;21:109-14.

THE ROLE OF SONOGRAPHY IN THE DIAGNOSIS OF TRAUMATIC RUPTURE OF THE ANTERIOR CRUCIATE LIGAMENT OF THE KNEE

Piyadara KHONGPIBOONKIT,¹ Chairat KHONGPIBOONKIT,²
Worachai AUEAPINUN,² Anun MALAIRUNGSAKUL²

ABSTRACT

OBJECTIVE: To evaluate the usefulness and value of sonography in the diagnosis of a rupture of the anterior cruciate ligament resulting from a recent knee injury, which was indicated by a physical examination suggesting of a traumatic anterior cruciate ligament injury.

MATERIALS & METHODS: Sonography was prospectively performed in 16 patients with a recent traumatic knee injury, in which a physical examination by an orthopaedist suggested a traumatic rupture of the anterior cruciate ligament of the knee. The presence of a hypoechoic collection along the lateral wall of the femoral intercondylar notch was interpreted as a hematoma together with a ligament stump at the femoral attachment of the anterior cruciate ligament. The operative findings were compared in 12 cases. Arthroscopy was subsequently performed in 2 cases.

RESULTS: The positive sonographic findings were confirmed by operative findings in 12 of 16 patients and the negative sonographic findings were confirmed by arthroscopy in 2 of 16 patients. In the remaining 2 of the 16 cases, there was a loss of follow up.

CONCLUSION: Sonography is a useful, available and inexpensive method of detecting the presence of a rupture of the anterior cruciate ligament, particularly in the hospitals which do not have MRI.

INTRODUCTION

In the hospitals which do not have advanced imaging machines such as magnetic resonance imaging, the patients with painful swollen knee after injury may present the primary care physician with diagnostic difficulties. Early clinical examination can be unreliable because of pain and poor muscle relaxation.¹ Sonography has a potential role as an inexpensive, available, sensitive and specific screening test to confirm the diagnosis of a rupture of the anterior cruciate ligament in those patients who

would benefit from specialist consultation and further investigation with magnetic resonance imaging.

The purpose of this study was to evaluate the accuracy, usefulness and value of sonography in the diagnosis of a rupture of the anterior cruciate ligament in the setting of a recent knee injury in which a physical examination by an orthopaedist suggested a rupture of the ligament.

¹Department of Radiology,

²Department of Orthopaedics, Phayao Hospital, Phayao, THAILAND 56000

MATERIALS AND METHODS

Sixteen patients with a history of traumatic knee pain within the preceeding 10 weeks, who were presented to one of the three orthopaedic surgeons and in whom the physical examinations suggested a traumatic anterior cruciate ligament rupture, underwent sonographic examinations of their injured knees.

The study group included 15 males and 1 female from 20 to 42 years of age. The sonographic examinations were done within one week of referral, usually on the same day. The physical examinations were done between 1 and 60 days after the knee injury, and then referred to the radiologist.

The sonographic examinations were done by the same radiologist.

The sonography was done with a real time 3535 B&K Medial Ultrasound machine using both a linear 7.5, 5.5 –MHz and a curved 3.5, 5.0-MHz transducer.

All patients were examined in the prone position with the posterior knee (popliteal) approach.

A transverse scan of the intercondylar notch was taken as the standard plane for the assessment of the anterior cruciate ligament.² The scan clearly showed both walls of the notch, the smooth hypoechoic concave synovium, and the popliteal artery lying just posterior to the lateral femoral condyle. The hypoechoic synovium, which is 2 – 3 mm. thick, lies parallel to the bony outline. Echogenic intercondylar fat lies centrally. (Fig 1, Fig 2)

The criteria for acute disruption of the anterior cruciate ligament in this study is the presence of a hypoechoic collection along the lateral wall of the femoral intercondylar notch with a convex medial border obscuring the covering synovium and displacing the intercondylar fat medially. The hypoechoic collection at the origin of the anterior

cruciate ligament is thought to represent a hematoma near the origin of the anterior cruciate ligament³ together with the anterior cruciate ligament stump in the cases of a complete tearing. (Fig. 3)

The hematoma size was measured at its maximum width in 2 planes at the femoral attachment of the anterior cruciate ligament.

The contralateral asymptomatic knee was examined in all cases.

The sonographic findings were confirmed by knee operation with anterior cruciate ligament reconstructions in 12 cases.

Arthroscopy was done in 2 cases

In two cases where patients had positive sonographic findings of a rupture of the anterior cruciate ligament, neither arthroscopy nor knee operation was done because of the patients did not come back to the hospital for further management.

RESULTS

The sonographic study showed a hypoechoic lesion at the origin of the anterior cruciate ligament in 14 patients. In 12 of these patients, the diagnosis was confirmed by knee operation and the surgical procedure was anterior cruciate ligament reconstruction. In the remaining 2 cases, the patients did not show up for further treatment.

2 of all 16 patients had negative sonographic findings. Arthroscopy was done and showed that the anterior cruciate ligaments were intact in both cases.

The average width of the hematoma in cases of anterior cruciate ligament rupture was 8 x 11.7 mm., and ranged from 4.7-15 mm. for the transverse plane and 7.5-20 mm. for the longitudinal plane.

The results of this study are shown in the table.

Case	Age in years / sex	duration A / B	US Findings	Size of the lesion. (mm.)	Treatment
1	37 M	1/1	Hypoechoic lesion at ACL origin, joint effusion.	4.7x11	Knee operation with ACL reconstruction
2	42 M	30/30	Hypoechoic lesion at ACL origin	8x12	Knee operation with ACL reconstruction
3	26 F	14/14	Fusiform hypoechoic lesion at ACL origin	5x16	Knee operation with ACL reconstruction
4	20 M	20/20	Hypoechoic lesion at ACL origin	10x12	Knee operation with ACL reconstruction
5	28M	5/5	Hypoechoic lesion at ACL origin	8x12	Knee operation with ACL reconstruction
6	26 M	1/10	Hypoechoic lesion at ACL origin	7.3x7.5	Knee operation with ACL reconstruction
7	30M	60/60	Hypoechoic lesion at ACL origin	15x20	Knee operation with ACL reconstruction
8	35M	2/2	Hypoechoic lesion at ACL origin	7x11	Knee operation with ACL reconstruction
9	20M	1/11	Fusiform hypoechoic lesion at ACL origin	5x8	Knee operation with ACL reconstruction
10	25 M	1/20	Hypoechoic lesion at ACL origin	6x8	Knee operation with ACL reconstruction
11	25 M	3/3	Hypoechoic lesion at ACL origin	10x12	Knee operation with ACL reconstruction
12	22 M	3/3	Soft tissue swelling; Joint effusion; No hypoechoic lesion at ACL origin	- -	Arthroscope-Intact ACL, Normal meniscus
13	22 M	1/5	Marked soft tissue swelling; Joint effusion; No hypoechoic lesion at ACL origin	-	Arthroscopy – Intact ACL
14	38 M	1/7	Hypoechoic lesion at ACL origin	9x10	Knee operation with ACL reconstruction
15	23 M	3/3	Hypoechoic lesion at ACL origin	11x15	Loss of follow up
16	27 M	2/2	Hypoechoic lesion at ACL origin	8x9	Loss of follow up

ACL = Anterior cruciate ligament.

M= Male

F = Female

Duration A/B = Duration of pain in days / Time from injury to sonographic examination in days.

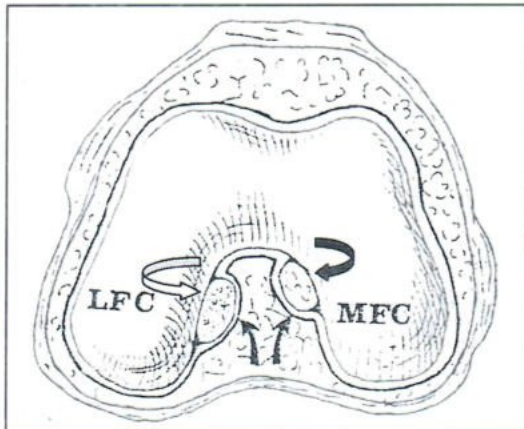
**Fig.1A**

Fig.1A Anatomic drawing shows femoral intercondylar notch in cross section. Anterior cruciate ligament(white arrow) originates from medial aspect of lateral femoral condyle (LFC). Posterior cruciate ligament(black arrow) lies against medial femoral condyle (MFC). A synovial membrane (curve black arrows) envelopes both ligaments.

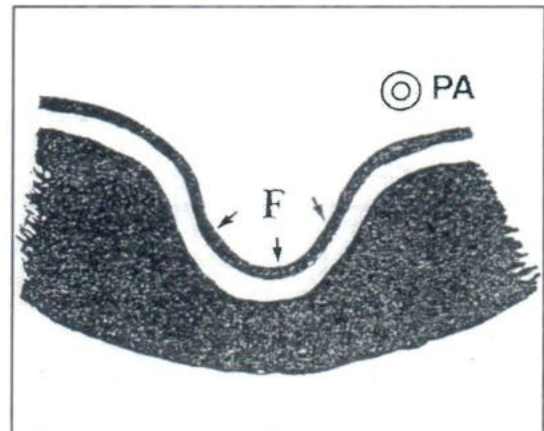
**Fig.1B**

Fig 1B Anatomic drawing of findings on transverse sonogram taken of region in A shows curves of femoral intercondylar notch, covering synovium(arrows),intercondylar fat (F) and popliteal artery (PA)

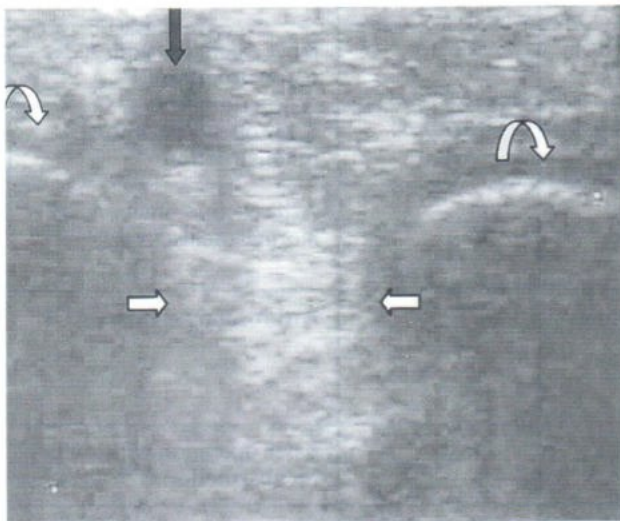
**Fig.2 A**

Fig.2 A A transverse scan of the intercondylar notch of **left** knee showed both walls of the notch (white arrows), the hypoechoic concave synovium (curve arrow), and the popliteal artery (black arrow).

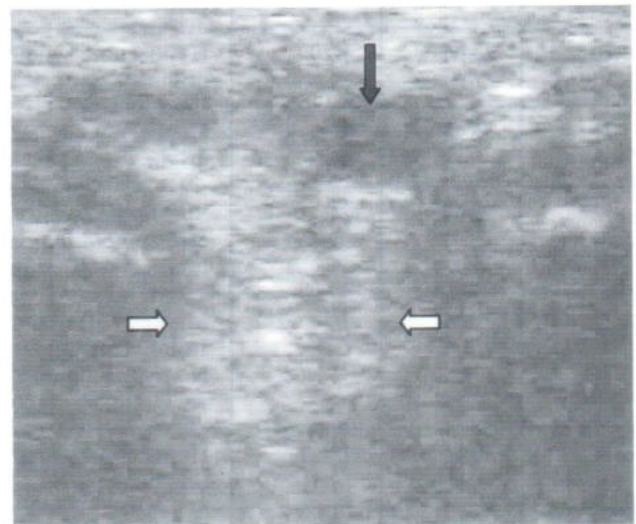
**Fig.2 A**

Fig.2 B A transverse scan of the intercondylar notch of **right** knee.

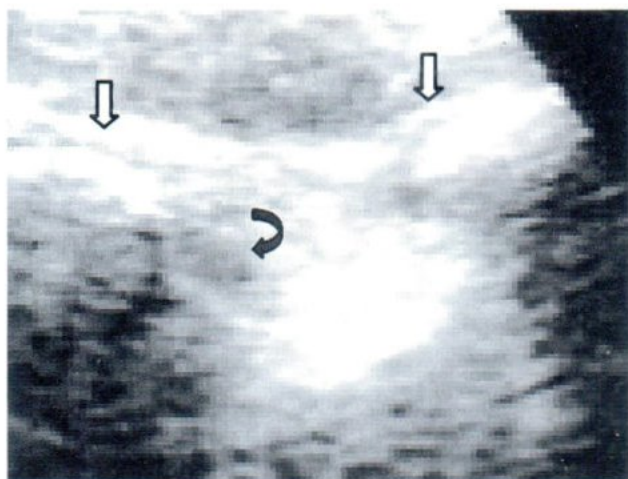
**Fig. 3 A**

Fig. 3 A Sonogram of case 5 shows a 8x12 mm. hypoechoic collection representing hematoma, at lateral wall of left femoral intercondylar notch (curved black arrow). Hypoechoic synovium lies parallel the femoral condyles (white arrows). Knee operation revealed ACL disruption at femoral attachment and a hematoma at ACL origin.

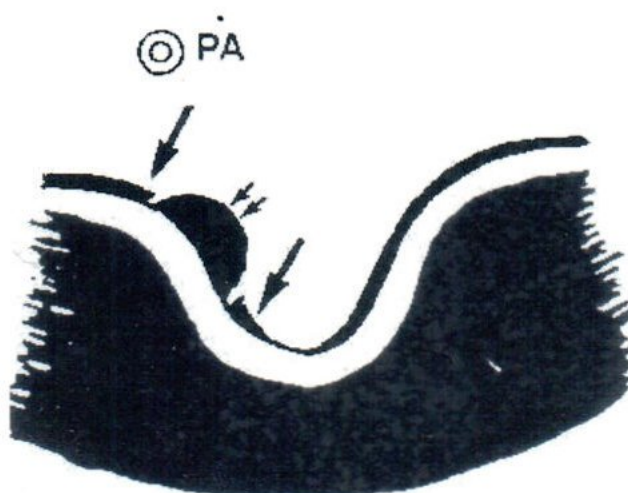
**Fig. 3 B**

Fig. 3 B Anatomic drawing of sonographic findings in A: Convex collection (small arrows) is hematoma at ACL origin. It obscures covering synovium (Large arrows)

PA = Popliteal artery.

ACL = Anterior cruciate ligament.

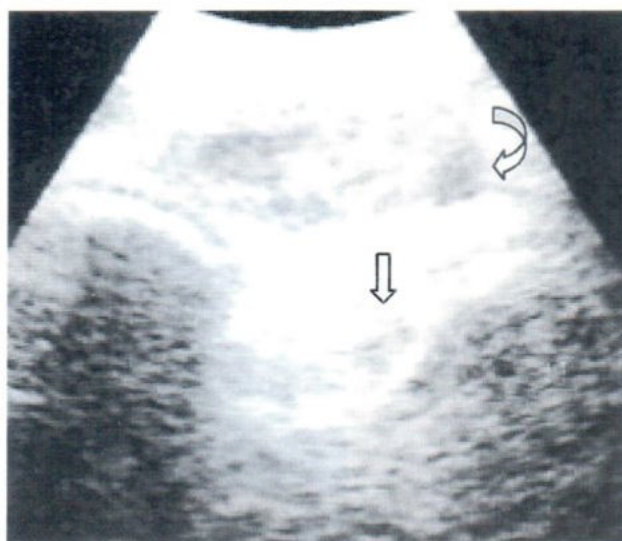
**Fig. 4 A****Fig. 4 B**

Fig. 4 Transverse scan of the intercondylar notch of patient number 14 showed no abnormal echogenicity of left knee (A). A hypoechoic collection (white arrow) at lateral wall of the femoral intercondylar notch of right knee represents hematoma at ACL origin.

Popliteal artery = curved arrow

ACL = Anterior cruciate ligament

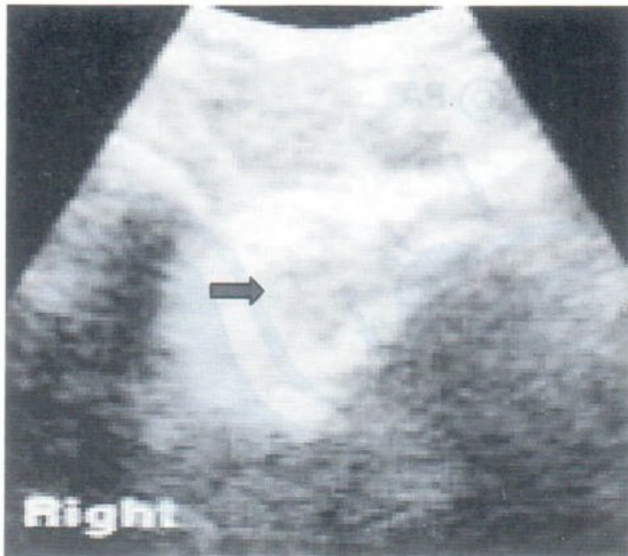
**Fig.5A**

Fig.5A Sonogram of case 7. showed a 15x20 mm. convex hypoechoic collection (black arrow) at the ACL origin of right knee, which was a hematoma together with a ligament stump. The sonographic finding was confirmed by knee operation.

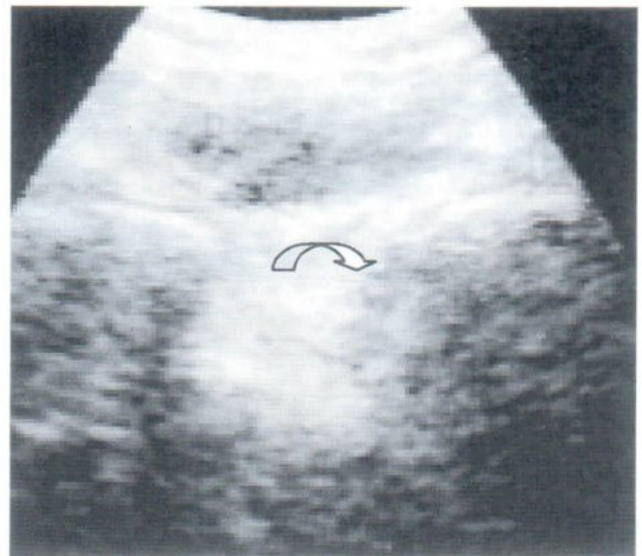
**Fig.5B**

Fig.5B Case 3. Sonogram of right knee showed fusiform hypoechoic collection (curved arrow) at lateral wall of the intercondylar notch and knee operation revealed midsubstance tear of the right ACL.

ACL = anterior cruciate ligament

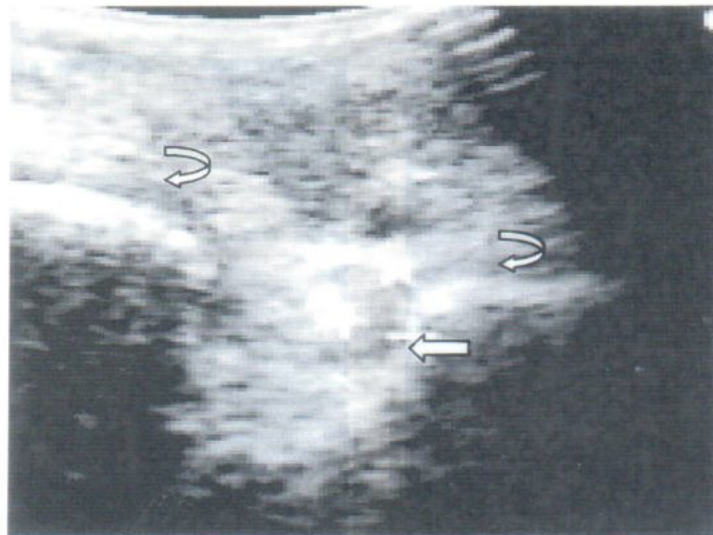


Fig.6 Case 1. Sonogram of right knee showed a 4.7x11 mm. hypoechoic collection at origin of right ACL (white arrow) and thickening of the hypoechoic synovium (curved arrow). The findings represented hematoma at ACL origin and joint effusion, respectively. Knee operation revealed midsubstance tear of right ACL and a hematoma at ACL origin.

DISCUSSION

The anterior cruciate ligament is approximately 38 mm. in length (range from 25 to 41 mm) with a width of approximately 1 cm. (range 7 to 12 mm). The anterior cruciate ligament has a synovial membrane envelope and is described as being intraarticular but extrasynovial. The anterior cruciate ligament arises from the posterolateral corner of the medial aspect of the lateral femoral condyle in the intercondylar notch. The tibial attachment/insertion is in a fossa in front of and lateral to the anterior tibial spine.⁴

Normally the anterior cruciate ligament is difficult to visualize sonographically.

The presence of a hypoechoic collection with a convex medial border obscuring the covering synovium and displacing the intercondylar fat medially was interpreted as indicating disruption of the anterior cruciate ligament. The hypoechoic collection, which is near the origin of the anterior cruciate ligament, is thought to represent a hematoma and the anterior cruciate ligament stump, the latter of which occurs in the cases of complete ligament tearing.

The presence of hematoma was found to be 100 % specific for the anterior cruciate ligament rupture.²

Most disruptions of the anterior cruciate ligament are either at the femoral attachment or midsubstance⁵; therefore the majority of the anterior cruciate ligament disruptions should be detectable with this sonographic technique. The disruptions occurring at the tibial attachment might not be detected with this sonographic technique because the hematoma might not be visible at the femoral origin.

The diagnosis of anterior cruciate ligament rupture by this sonographic technique is therefore an indirect method, relying on visualizing the hematoma

that occurs as a result of anterior cruciate ligament disruption rather than the disrupted ligament itself.

The sensitivity, specificity, positive predictive value and negative predictive value were not calculated in this study because of the small number of patients (16 patients). Further study with more collected patients is required to determine the accuracy of sonography in the diagnosis of anterior cruciate ligament rupture.

In conclusion, sonography is a very useful method of examination to confirm the diagnosis of disruptions of the anterior cruciate ligament in patients with a recent knee injury which was indicated by a physical examination suggesting a traumatic anterior cruciate ligament rupture. Sonography is an available and inexpensive adjunct in the assessment of patients with an acute knee injury, particularly in hospitals which do not have magnetic resonance imaging. This sonographic technique could significantly help orthopaedic surgeons to confirm their diagnoses and enable them to do further management such as anterior cruciate ligament reconstruction without further investigation by MRI.

REFERENCES

1. Noyes FR, Bassett RW, Grood ES, Butler DL. Arthroscopy in acute traumatic hemarthrosis of the knee: incidence of anterior cruciate tears and other injuries. *J Bone Joint Surg Am* 1980; 62-A: 687-695
2. R. Ptasznik, J Feller, J Bartlett, G. Fitt, A. Mitchell, O. Hennessy. The value of sonography in the diagnosis of traumatic rupture of the anterior cruciate ligament of the knee. *AJR* 1995; 164: 1461-1463
3. Berquist TH, Ehman LE. The knee. In: Berquist TH, ed. *MRI of the musculoskeletal system*. New York: Raven, 1990: 195-251

4. Charles A. Rockwood, Jr, Devid P. Green, Robert W. Bucholz. Injuries of The Cruciate Ligaments. Fractures in Adults, 3rd ed. New York : London, 1991 ; 1865 – 1885
5. Peagin JA, Abbott Hg, Rokus JR. The isolated tear of the anterior cruciate ligament. J Bone Joint Surg Am 1972 ;47-A : 1340-1341
6. Van Holsbeek M, Introcaso JH. Musculoskeletal ultrasound, 1st ed. St. Louis: Mosby, 1991 : 300-308

INTER-COMPARISON OF ACQUISITION AND PROCESSING SOFTWARE FOR MUGA STUDY AND PIP

Chatchai NAVIKHACHEEVIN, M.Sc.

ABSTRACT

Software quality assurance in nuclear medicine can be performed by software phantom if the system has the universal interface. Patient file data from a particular computer system may be converted into the standard interfile format, and subsequently converted from interfile format to the specific file format of another computer system. If the system has no interfile option, hardware phantom must be used to validate the accuracy of the software analysis result. The dynamic cardiac phantom was used to verify both acquisition software and analysis software. This make it more importance to guarantee quality and reliability in multi-gated acquisition (MUGA) study. The data set from GE was used to analyze on Trionix and PIP (Portable Image Processing) software. The result shown that GE and Trionix were not different but PIP will give low ejection fraction (EF) than those two systems.

INTRODUCTION

The quality of nuclear medicine imaging depends on the whole investigation procedure.¹ If any of the different steps is unsatisfactory, the result is not reliable. In 1988, COST B2 (Cooperation in the field of Scientific and Technical research) project with the objective of establishing some software quality assurance programs for nuclear medicine software was being formulated in Europe.² More recently, the growing interest in software quality assurance has increased the demand for exchange of image data between systems in order to compare the results yielded by applications programs to measure the same parameters.^{3,4} Some computer vendors supply utility program to facilitate image file transfer from another format to their own.

The exchange of nuclear medicine image file between difference computer systems is one of the main immediate issues of the project. Crucial problems lie not with image exchange itself but with

exchange of the administrative and total file content, since each manufacturer has a unique file structure. The concept of a standard format intermediate file (interfile) is using ASCII key-value pairs for storage of administrative data parameters (*.hdr), and a purely binary data file (*.img).^{5,6} Patient file data from a particular computer system may be converted into the standard interfile format, and subsequently converted from interfile format to the specific file format of another computer systems. In this way, patient data may be transferred to any computer system by using only a single interfile read and write program for each type of computer system. Storage of software phantoms in interfile can then be made on any standard removable storage media, for example MS-DOS formatted floppy disks used for PCs.

A software phantom is a set of real or pseudo data, or a mathematically derived set of data that can be formatted into the equivalent of a patient data file,

for purposes of validation of analysis software.⁷ Such data sets cannot be used to validate the acquisition software. A pseudo patient data set is usually obtained from some simple physical model or phantom. More complex software phantoms may be derived from data collected from phantoms with mechanical motion such as various type of cardiac phantom. The advantage that such phantoms offer is that the condition of data collection may be rigidly controlled and the acquisition software may be tested. On the other hand, The phantom of this nature cannot be expected to simulate all conditions likely to be encountered in clinical practice.

In order to validate software on different systems, it is desirable to use the same software phantom in each case. Unless the same input data are used in each case, it is impossible to determine if variations are due to differences in the data or in the analysis software. Transfer or interchange of software phantoms between systems has a number of associated problem which arise at different level, media interchange, file structures and incomplete data. The

objective of this study is to perform an inter-comparison of the three systems processing program for left ventricular ejection fraction (LVEF) using a single operator and image data transfer between systems.

MATERIALS AND METHODS

The Veenstra dynamic cardiac phantom model DCP 101 was used to provide identical data between GE (Camstar) and Trionix (Triad) SPECT system.⁸ The phantom consists of two compartments, one of which (Fig. 1) is fixed and simulates the background areas (lung, left atrium, aorta, liver and spleen). The other compartment (Fig. 2) has a hollow chamber which simulates the left ventricle and right ventricle. Both compartments were filled with a homogeneous mixture of Technetium-99m, 111 Mbq for background compartment and 37 Mbq for ventricle compartment. The movement of metal jaws (Fig. 3) will attenuate the peripheral activity of the cardiac chamber and synchronize to the electrical output to the R-wave trigger.



Fig.1 A hollow background chamber simulates atrium, aorta, liver and spleen

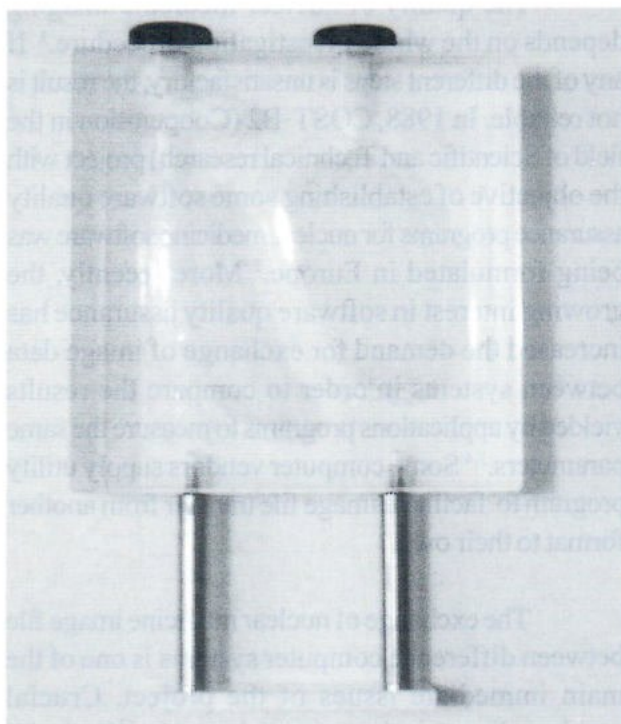


Fig.2 A hollow cardiac chamber that represents the RV and LV



Fig.3 Metal jaws to simulate the beating heart

The three presets EF of 30%, 60% and 80% and heart rate 40, 80 and 160 beet/min were used for MUGA data acquisition. The acquisition matrix 64x64, 24 frames for each cycles, acquisition time

10 min, zoom 2.67 and LEGP collimator was used for GE Camstar (Fig.4) and zoom 1.6, LEUR collimator was used for Trionix Triad (Fig. 5).

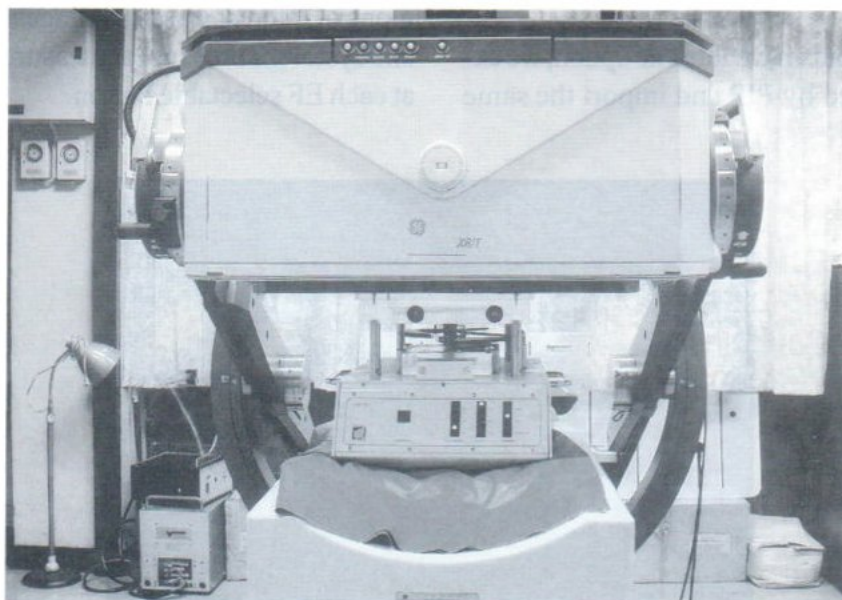


Fig.4 Data acquisition on GE Camstar

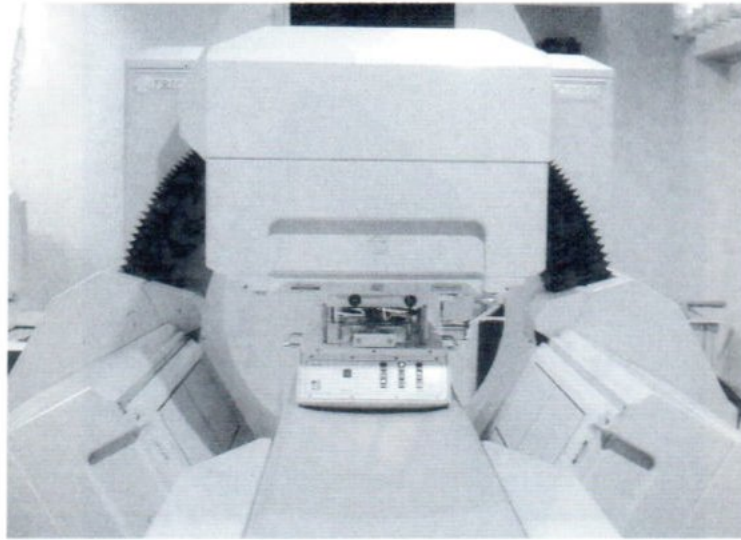


Fig.5 Data acquisition on Trionix Triad

The acquisition data from GE and Trionix were analyzed both manual and semi-automatic methods. With some help of GE Camstar maintenance service officer to read and write GE Camstar data file on personal computer (PC), we can use ImageJ program to open file and save as image file (*.img). We created header file (*.hdr) as interfile version 3.3 format and analyzed these data on PC by PIP (Portable Image Processing) software.

Because Trionix have Interfile option, we export data to analyzed by PIP and import the same

data back to Trionix again to analyze by semi-automatic method.

With the background chamber removed, the movable jaws were first set at the widest position (end-diastole) and static image was acquired for 1 minute, then at closed position (end-systole) and acquired static image again. Perform the same at each preset selectable to determine EF by drawing regions of interest on static images (Fig.6) at diastole and systole. Three repeat measurements were made at each EF selectable button.



Fig.6 Static images from GE used to draw ROI to calculate EF

STATISTIC ANALYSIS

The paired-sampled t-test was used to compare means of ejection fraction between static and MUGA acquisition. $P < 0.05$ was considered statistically significant.

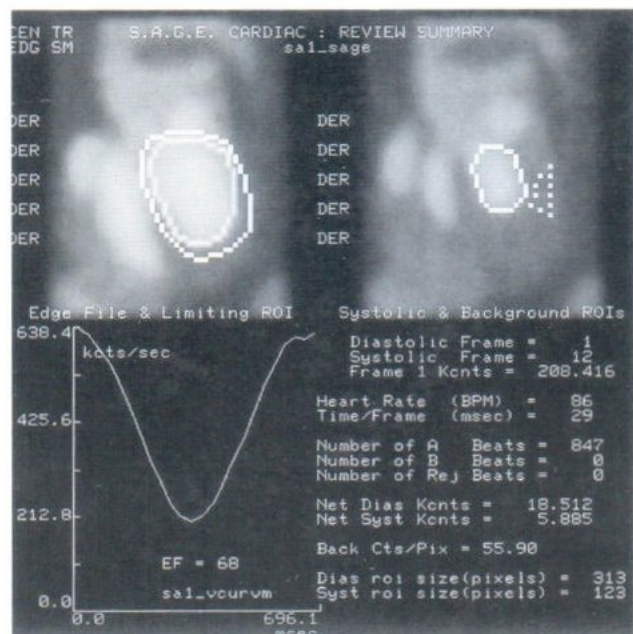


Fig. 7 GE semi-automatic method at HR 80 and EF 60

RESULTS

The results on LVEF in percent was recorded in Table 1 acquired by GE Camstar, using semi-automatic (Fig.7) and manual (Fig.8) modes compared to analyze by PIP (Fig.9).

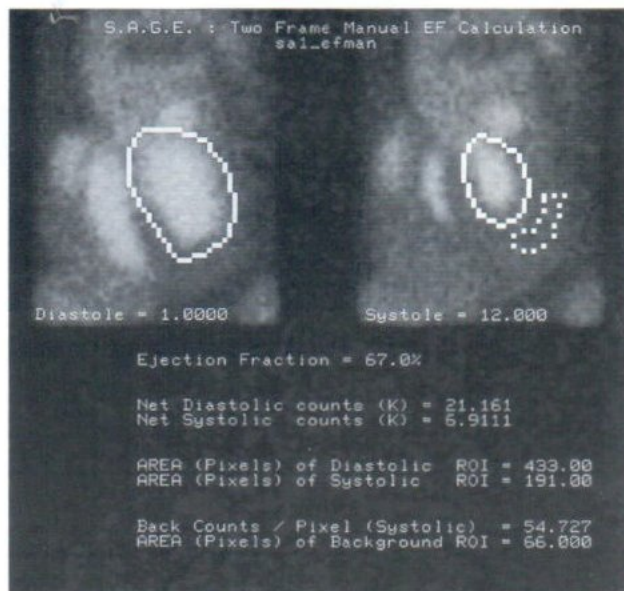


Fig.8 GE manual 2 frame method at HR80 and EF60

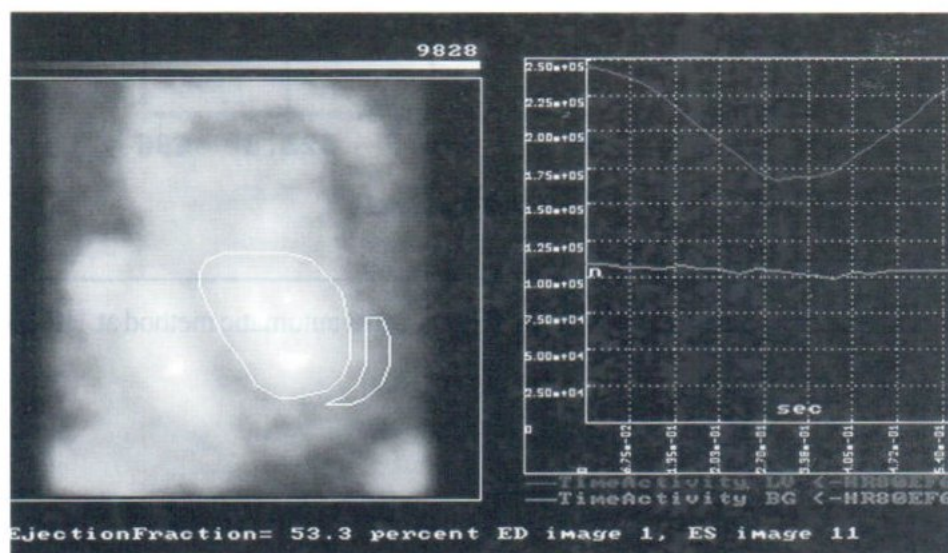


Fig. 9 GE data at HR80 and EF60 analyzed on PC with PIP

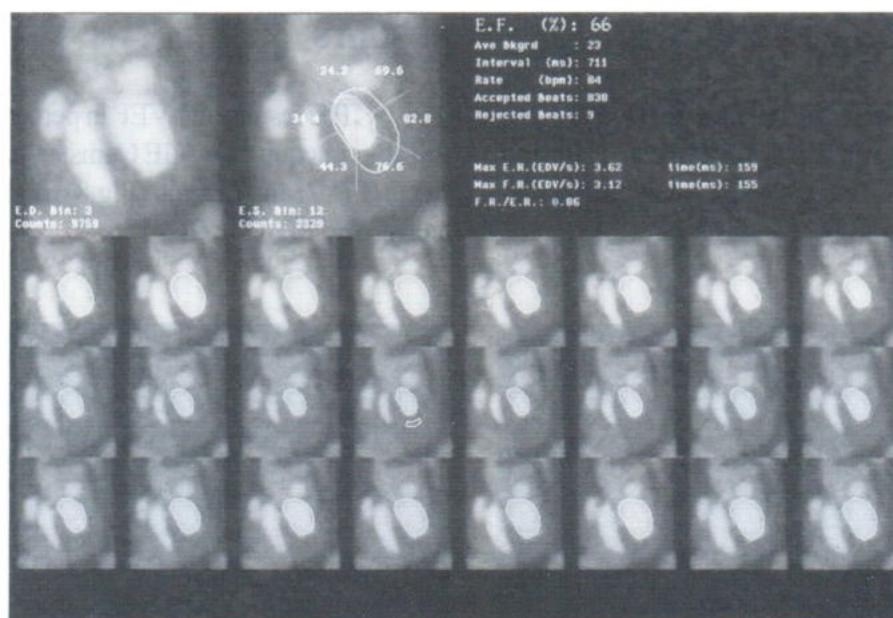


Fig.10 Trionix semi-automatic method at HR80 and EF60

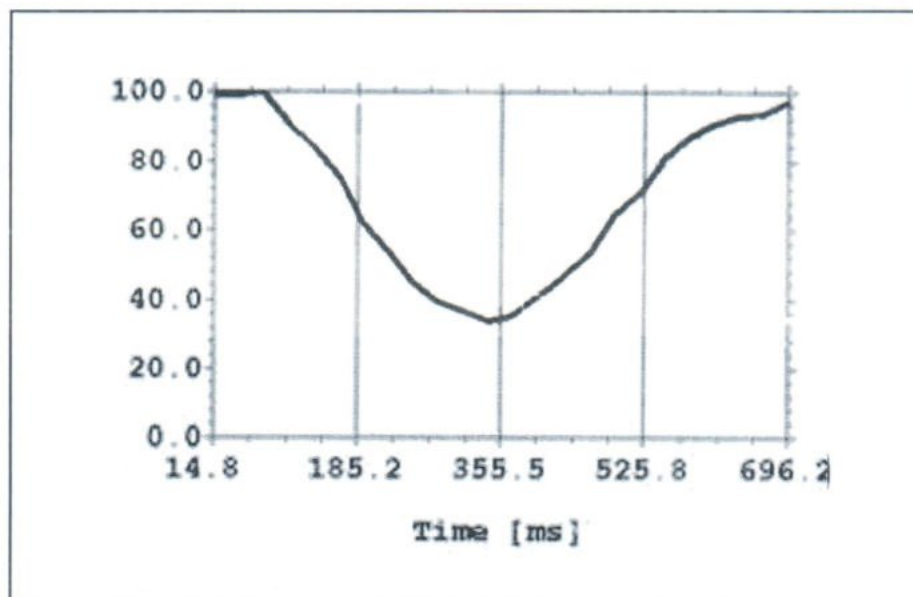


Fig.11 Time activity curve from Trionix semi-automatic method at HR 80

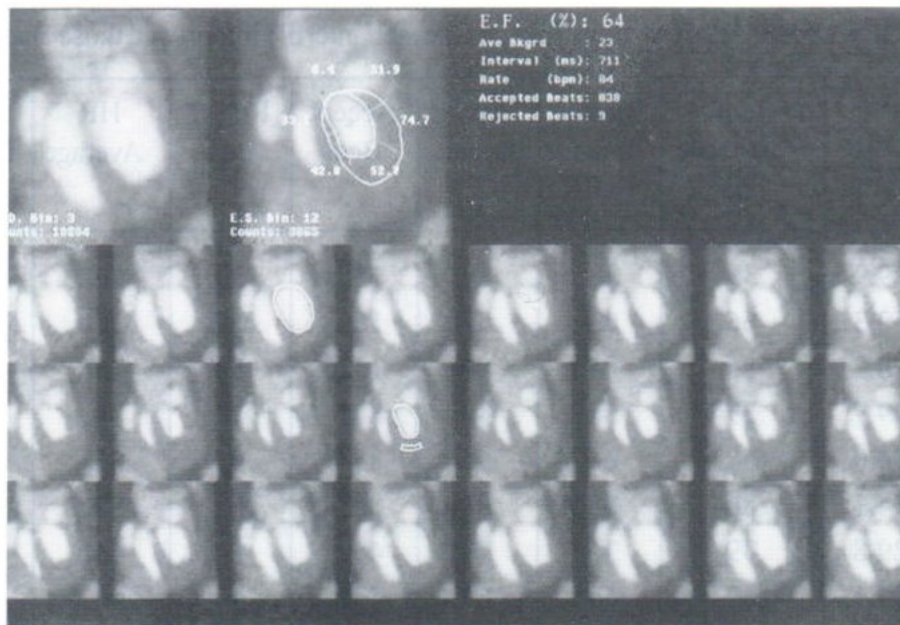


Fig.12 Trionix manual 2 frame method at HR80 and EF60

The results on LVEF in percent was recorded in Table 2 acquired by Trionix Triad, using semi-automatic (Fig.10-11) and manual (Fig12) modes compared to analyze by PIP.

GE data in form of interfile format was send

from PC to analyzed on Trionix via network. The result was given on Table3 compared to GE and PIP.

The mean results from static image at each EF from both system was record on Table 4 compared to the MUGA data at same EF.

Table 1 The result of MUGA analysis from GE data and those analyzed on PIP

Veenstra	PIP %EF	Semi Automatic %EF	Manual 2Frame %EF	Accept Beat	Reject Beat	HR Average	ED Frame No.	ES Frame No.
HR160EF30	30.5	44	43	1541	48	166	1	12
HR160EF60	55.5	69	68	1549	44	166	1	13
HR160EF80	72.8	86	85	1541	35	166	1	11
HR80EF30	30.4	42	42	842	0	86	1	13
HR80EF60	53.3	68	67	847	0	86	1	12
HR80EF80	72.4	85	85	834	0	86	1	12
HR40EF30	30.7	41	41	486	1	49	1	12
HR40EF60	54.8	67	67	481	0	49	1	11
HR40EF80	73.4	84	83	486	0	49	1	11

Table 2 The result of MUGA analysis from Trionix data, self interfile import and those analyzed on PIP

Veenstra	PIP %EF %EF	Semi Automatic %EF	Manual 2Frame %EF	Interfile Import %EF	Accept Beat	Reject Beat	HR Average	ED Frame	ES Frame
HR160EF30	29.9	39	38	39	1591	30	162	2	12
HR160EF60	52.3	66	63	67	1578	12	159	1	12
HR160EF80	78.9	86	84	86	1528	58	158	2	12
HR80EF30	29.7	39	38	39	875	1	86	1	12
HR80EF60	54.0	68	64	66	838	9	84	1	12
HR80EF80	74.1	86	83	85	827	5	82	1	12
HR40EF30	29.8	39	36	40	460	1	45	1	11
HR40EF60	57.1	67	66	67	462	4	46	1	12
HR40EF80	74.0	85	84	87	483	4	48	2	11

Table 3 Inter-comparison of analysis software by using data set from GE and those analyzed on Trionix and PIP (%EF)

Veenstra	GE (Original)	Trionix	PIP
HR160EF30	44	43	30.5
HR160EF60	69	71	55.5
HR160EF80	86	87	72.8
HR80EF30	42	41	30.4
HR80EF60	68	70	53.3
HR80EF80	85	86	72.4
HR40EF30	41	41	30.7
HR40EF60	67	70	54.8
HR40EF80	84	86	73.4

Table 4 The mean %EF from static image and MUGA at each preset button (mean±s.d.)

Veenstra	Mean Static GE	Mean Static Trionix	Mean MUGA GE Trionix (Semi)	Mean MUGA on (Semi)	Mean GE on PIP	Mean Trionix PIP
EF30	39.3±0.2	36.4±1.1	42.3±0.2	39.0±0.0	30.5±0.2	29.8±0.1
EF60	66.8±2.8	65.3±1.3	68.0±1.0	67.0±1.0	54.5±1.1	54.5±2.4
EF80	88.3±0.6	83.3±0.2	85.0±1.0	85.7±0.6	72.9±0.5	75.7±2.8

DISCUSSION

Table 1 and 2 shows that heart rate detection on GE is more stable than Trionix. At high heart rate more rejected beat is observed compare to low heart rate on both system. This may be due to electrical noise of the system. The heart rate have no effect on EF. No differences between Semi-automatic and Manual 2 frames method. End-diastolic frame were major on frame number 1 but end-systolic was different in ± 1 frame between two systems.

Table 2 show that Trionix import interfile have no effect on result ($p = 0.782$) compared to original data, but rejected beat will be set to zero. Trionix edge detection algorithm was not correct in some frame. So, operator must adjust it by manual, frame by frame. Trionix can not change diastolic and systolic frame by manual method as compare to GE. These two frames were detected by oval ROI on LV. This may be missing some part of LV due to Oval shape and wrong detection frame may occur.

The acquisition data from dynamic cardiac phantom and analyzed by its own semi-automatic algorithm had shown no significant differences between GE and Trionix ($P = 0.12$). When we analyzed both data on PIP, lower EF was observed with significant ($p < 0.001$) differences compared to original system. This may be due to differences in algorithm because PIP used fix ROI but GE and Trionix used varied ROI according to the edge of LV.

Table 3 shows inter-comparison analysis software by using GE data when analyzed on Trionix having no significant changes ($p = 0.067$) but having significant changes on PIP ($p < 0.001$)

Static image was used to perform calibration of pre-set button value. Table 4 show that no significant differences on MUGA from GE ($p = 0.746$) but significant differences on MUGA from Trionix ($p < 0.001$). This may be due to very small matrix as MUGA is using and error on drawn ROI because

image was very small.

When we used Veenstra dynamic cardiac phantom, parallel plane must be strictly checked between phantom and detector. Wrong results may be due to geometrical error. However, pre-set EF value may be adjusted by means of multiturn potentiometers so that a wide range of EF values may be simulated. This phantom was easy to be used, simple to be operated but relatively heavy.

CONCLUSION

The acquisition MUGA on both GE and Trionix give the same result. PIP software will give lower EF with significant change due to calculation algorithm. This GE MUGA data had been validated and can be used as software phantom. Interfile is a software package which is more helpful to share data and compare results between analyzing systems in nuclear medicine. It is available to communicate in interfile format from center to center via network. Software phantom may be useless if that system has no this option, especially the old camera system. Hardware phantom will be needed in this case. Quality assurance in nuclear medicine software must be performed to guarantee quality and reliability.

ACKNOWLEDGEMENT

I would like to thank Dr. Andrew Todd -Pokropek to allow me to used PIP software, Mr. Samarn Limpkittisin who convert GE MUGA data to PC and Dr. Anchali Krisanachinda to advocate and comment this research.

REFERENCES

1. Coakley AJ. Quality assurance in nuclear medicine. *Nuc Med Commun* 1989; 10: 139-140.

2. Cosgriff PS. COST B2 final report Quality assurance of nuclear medicine software. Luxembourg: European Communities, 1997: 11-14.
3. Craddock TD, Bailey DL, Hutton BF, de Conninck F, Busemann Sokole E, Bergmann H, Noelpp U. A standard protocol for the exchange of nuclear medicine image files. *Nuc Med Commun* 1989;10:703-713.
4. Makler, Jr PT, McCarthu DM, Bergey P, Marshall K, Bourne M, Velchik M, Alavi A. Multiple hospital survey of ejection fraction variability using a cardiac phantom. *J Nucl Med* 1985;26:81-84.
5. Britton KE, Busemann Sokole E. Quality assurance in nuclear medicine software and 'COST'. *Nuc Med Commun* 1990; 11: 334-338.
6. Maguire, Jr GQ, Noz ME. Image formats: Five years after the AAPM standard for digital image interchange. *Med Phys* 1989; 16(5): 818-823.
7. Craddock TD, Busemann Sokole E, Erickson JJ. Development of software phantoms for software validation. In: *Dynamic functional studies in nuclear medicine in developing countries*. IAEA, Vienna, 1989:483-492.
8. Busemann Sokole E, Craddock TD. The use of phantoms for quality control in gated cardiac studies. *J Nucl Med Technol* 1985;13:5-10.

LARGE PAPILLARY CARCINOMA OF URINARY BLADDER

Siriporn POOLSIRI¹ MD., Chakrit HEKPHEERA² MD.

ABSTRACT

A case of large papillary carcinoma (low grade) of urinary bladder was presented. The patient is a prisoner, referring from a nearby prison with a history of chronic gross hematuria, dysuria, more frequent urination and a sense of incomplete emptying of the bladder after urination, so that sometime he had to force out or compress the suprapubic area to increase urination. Multi-modality imagings (retrograde urethrogram, sonogram, CT whole abdomen) were performed and revealed multiple large polypoid masses projected out from bladder wall into the bladder capacity. The presumptive diagnosis was rhabdomyosarcoma or myoma. He was treated by total cystectomy and ileal conduit. The pathologic diagnosis was multiple large papillary carcinoma, low grade, of urinary bladder (greatest diameter of the tumor was 11 cm.)

CASE REPORT

A 32-year-old Thai man was referred from a nearby prison hospital to urology division, surgery department with symptoms of progressive hematuria, dysuria, more frequent urination, sense of incomplete emptying of the bladder after urination and sometime he had to force out or compress the suprapubic area to increase urination. He was treated as urinary infection about 3 year. To rule out urethra stricture, retrograde urethrogram (RP) was done (fig. 1a, 1b) and reveal mild to moderate narrowing of the membranous and prostatic part of the urethra with an evidence of large areas of filling defect, as round masses, in the bladder cavity.

Additional sonogram was done and confirmed the finding of multiple round soft tissue masses. (Fig. 2a and 2b) Following of computerized tomography (CT.) of the whole abdomen (Fig. 3a, 3b, 3c), it showed multiple mild enhancing rather round masses

pedunculated from lateral and posterior wall of the bladder, varying in sizes about 3-8 cm with thickened of bladder wall and mild bilateral hydronephrosis. He was received transurethra resection of bladder tissue and pathologic diagnostic was papillary carcinoma invading the lamina propria. So the definite treatment was radical cystectomy with ileal conduit and to be followed up every 3 months in the first year.

Pathologic diagnosis;

- Large papillary carcinoma, low grade, of urinary bladder (greatest diameter of tumor 11 cm.)
- Tumor invades lamina propria
- No invasion of muscularis propria of bladder wall
- Chronic cystitis with hypertrophy of muscular layer together with focal fibrosis
- No evidence of metastasis to lymphnode, ureter, urethra, prostate gland and seminal vesicles.

¹ Department of Radiology , Pranangkla Hospital , Nonthaburi , Thailand.

² Department of Surgery , Division of Urology , Pranangkla Hospital , Nonthaburi , Thailand.

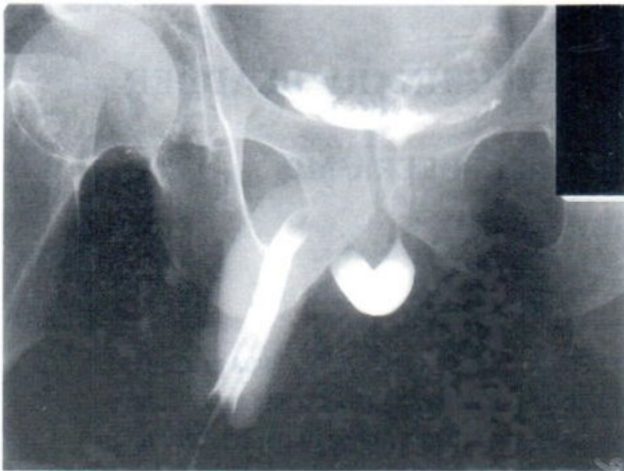


Fig. 1a,1b Retrograde urethrogram 1 a, mild to moderate narrowing of membranous and prostatic part of urethra.



Fig. 1b, Large number of filling defects looking like round masses in the bladder cavity

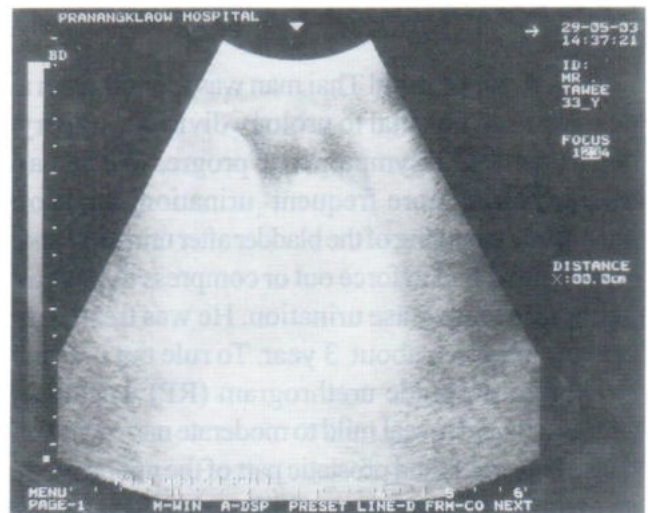
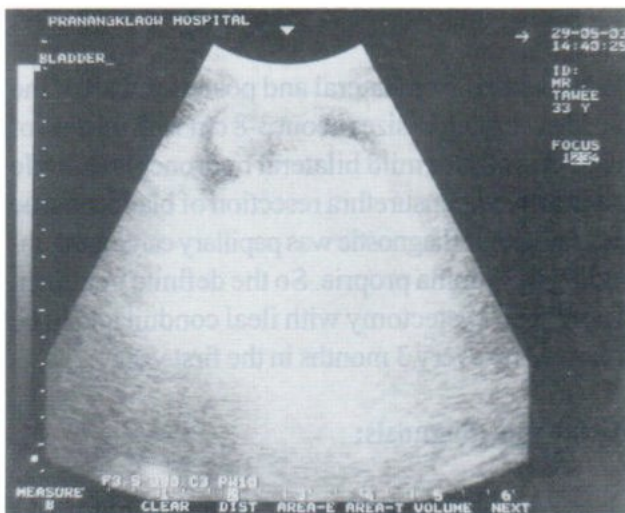
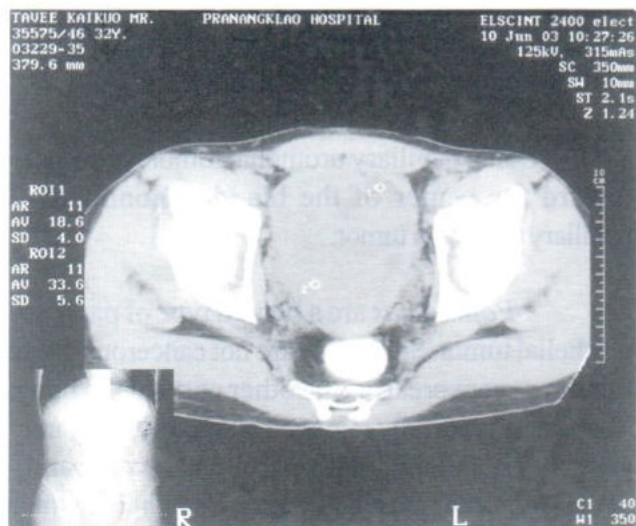
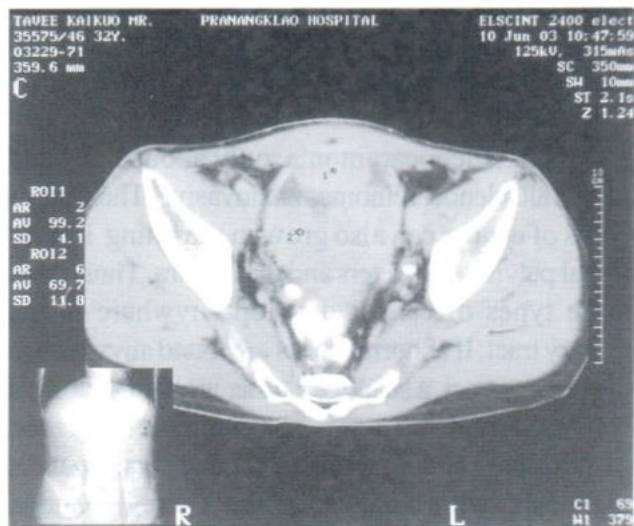


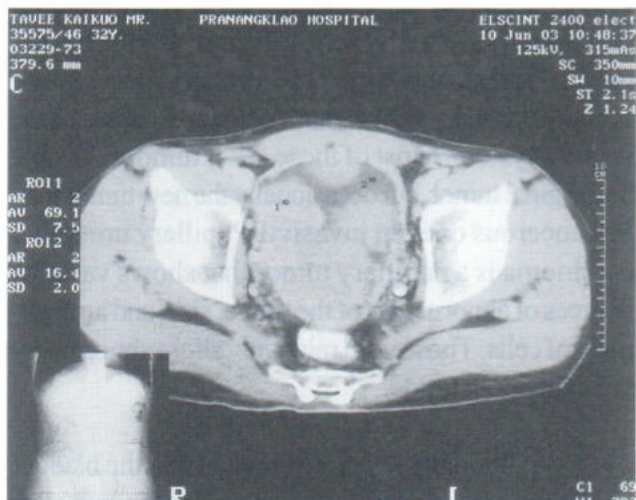
Fig. 2a,2b Ultrasonogram Multiple round soft tissue masses in the bladder cavity.



3a



3b



3c

Fig. 3a,3b,3c CT. whole abdomen multiple mild enhancing rather round masses pedunculated from lateral and posterior wall of bladder, varying in size 3-8 cm., with thickening of bladder wall

DISCUSSION

The bladder is a hollow pelvic organ that collects and stores urine produced by the kidneys. The wall of bladder has several layers

1. urothelium or transitional epithelium (urothelial cell or transitional cells), lines the inside of the kidney, ureter, bladder and urethra.

2. lamina propria thin zone of connective tissue, beneath the urothelium.

3. muscularis propria, the next deeper area, muscular tissue.

4. fatty connective tissue, beyond the muscle to separate the bladder from other nearby organs.

Type of bladder cancer, the main 3 types are

1. Transitional cell carcinoma (urothelial carcinoma), is the most common form of bladder cancer, more than 90% of bladder cancer

2. Squamous cell carcinoma, about 2-3% and nearly all squamous cell carcinomas are invasive

3. Adenocarcinoma, only about 1-2% and nearly all adenocarcinomas are invasive. These same types of cancer can also grow in the lining kidney (renal pelvis), the ureters and the urethra. Thus, these three types of cancer develop anywhere in the urinary tract. If abnormal cells are found anywhere in the urinary tract, a search for other areas of abnormal cells is warranted. Therefore, a complete evaluation of the urinary system is recommended for the patient diagnosed with a cancer of the kidney, bladder, ureter, or urethra.

Rhabdomyosarcoma is very rare cancer that affects other tissues and organs more than the bladder. It usually affects infants and is seldom found in adults.

Sub- Types of Urothelial tumor.

- *Noninvasive urothelial tumors*; The cancer is only in the inner most layer of the bladder, the urothelium, not spreading to deeper layers of the bladder.

- *Invasive urothelial tumors*; The cancer has spread from the urothelium to the deeper layers of the bladder wall and it is very important to determine exactly how far into the bladder wall that the cancer has invaded. Invasion of the thick, deep muscle layer is much more serious than invasion that limited to the superficial connective tissue (lamina propria) or the superficial, thin, muscle layer (muscularis mucosae)

- *Superficial urothelial tumor*; This category includes bladder cancers that are non invasive as well as invasive cancers that have not spread deeply into the bladder wall (only lamina propria). If a cancer has invaded the bladder's main muscle layer, it is not considered superficial.

- *Papillary urothelial tumor*; papillary

tumors have slender finger-like projections that grow into the hollow center of the bladder.

Some papillary urothelial tumors grow only toward the center of the bladder, noninvasive papillary urothelial tumor.

* *Papillomas* are a benign type of papillary urothelial tumor. Since they are not cancerous, these tumors never spread to the other parts of the body. They are successfully removed by surgery, and rarely grow back. Patients with papillomas very rarely develop another papillary tumor elsewhere in their urinary system. Papillary urothelial neoplasms of low malignant potential are tumors that are usually successfully treated by surgical removal. But, it is not unusual for patients with these tumors to develop one or more papillary tumors later on in other areas of the urinary system. Most of these other tumor resemble the original tumor, but occasionally the new tumor may be cancerous or even invasive. Papillary urothelial carcinoma is a papillary tumor that shows variable degrees of abnormality of the shape, size, and arrangement of cells. Those with relatively slight abnormality are called low grade.

Although they rarely invade into the bladder wall, they often return with urinary symptoms after surgery. Carcinomas with greater abnormalities, called high grade carcinomas, are more likely to invade into the bladder wall or even spread to other parts of the body.

Some papillary carcinomas grow inward toward the bladder wall and also grow outward into the bladder cavity, called invasive papillary urothelial carcinomas or cancers.

-Flat urothelial tumor;

flat urothelial carcinomas do not grow toward the hollow part of the bladder at all. Some of these only involve the layer of cells closest to the inside or the hollow part of bladder, called noninvasive flat

urothelial carcinoma or flat carcinoma in situ (CIS). Some flat urothelial carcinomas invade the deeper layers (away from the hollow part) particularly the muscle layer, called flat invasive urothelial carcinomas.

SYMPTOM

Early recognition of symptoms; hematuria (microscopic or gross), more frequency of urination with a sense of incomplete emptying of bladder after urination, pain on urination (dysuria) or force out urination.

The symptoms for bladder cancer are not specific, inflammatory condition may cause similar symptoms.

Diagnosis; We have several diagnostic tool including radiology, cystoscope and pathology. However, a definitive diagnosis of bladder cancer can only be made by bladder tissue diagnosis.

Radiological diagnosis including several methods started from, conventional x-ray; intravenous pyelogram (IVP), retrograde pyelogram, cystogram, Computerized Tomogram (CT.) Megnetic resonance. Imaging (MRI) Cystoscopy was started by urologist, for direct visual examination and for biopsy bladder of the tissue.

Pathologist, to identifies whether the tumor is benign or malignant and the type of tumor. This is essential because tumors of different types behave very differently and require different treatment regimens.

TREATMENT

Treatment of transitional cell or urothelial carcinoma is different for superficial tumors and muscular invasive tumors. Superficial bladder cancer can be managed without cystectomy, usually by tranurethral resection (TUR) with or without

adjuvant intravesicle radiotherapeutic implantation by Au¹⁹⁸ or Ta¹⁸² or intravesical chemotherapy. Muscular layer invasive tumors require cystectomy. The distinction between superficial bladder cancer and muscle invasive bladder cancer is critical and the choice of treatment can be discusse in a tumour clinic which consisted of a urologist, a pathologist, a radiotherapist and a chemotherapist.

CONCLUSION

Papillary carcinoma of urinary bladder is a sub-type of urothelial tumor or transitional tumor, which is the most common form of bladder cancer, it shows slender finger-like projections that grow into the hollow center of bladder. It can be noninvasive or invasive bladder cancer. In this reported case, he is a prisoner that has progressive gross hematuria and symptoms of partial lower urinary tract obstruct for a long time, so multiple large papillary tumor masses are demonstrated.

REFERENCE

1. Anderstrom C, Johnson S, Nilsson S. The significance of lamina propria invasion on the prognosis of patients with bladder tumor. *J Urol* 1980;124 (1) : 23-26
2. Shaul G. Massry, Richard J. Glassock: Neo plastic disease of the pelvis, ureter, bladder and urethra, Textbook of Nephrology, Fourth edition : 1051-1058, 2000
3. Henly NM, Ahmed S, Flangan MJ, etal. Superficial bladder cancer: progression and recurrence. *J Urol* 1983; 130(6) 1083-1086
4. Lantz EJ, Hattery RR. Diagnostic imaging of urothelial cancer. *Urol\clin\north Am* 1984; 11(4) 567-583
5. David M. Witten, George H. Myers Jr., David C. UTZ, Tumor of The genitourinary tract, Emmett's Clinical urography : An Atlas and Textbook of Roentgenologic Diagnosis, Fourth edition : 1618-1641, 1977

6. Walsh, Patrick C., Transitional cell cancer : upper tracts and bladder, Radiology of urinary tract, Cambell's Urology, Fifth edition : 1343-1425, 312-336, 1986
7. Althausen, A.F., Prout, G.R. , Jr., and Daly, J.J. : Noninvasive papillary carcinoma of the bladder associated with carcinoma in situ, J. \urol. 16-575, 1976
8. Mostofi, F.K.: Cancer of the urinary bladder – Epidemiology and aetiology Urol. Res., 6-183 , 1978
9. Mostofi, F.K.: Pathology and sprad of carcinoma of bladder. JAMA , 206, 1968

HEMOPTYSIS CAUSED BY A MIGRATORY K-WIRE: A case report and review literature

Nitaya THONGSIBKAO, M.D.¹

ABSTRACT

A case of the migratory Kirschner wire (K-wire) from right clavicle to trachea, causing hemoptysis was diagnosed in 47 year-old man. Plain film, CT scan and esophagography were illustrated. Surgical removal of K-wire was done and the false aneurysm of thyrocervical trunk was seen during surgery.

Key words : Kirschner wire, K-wire, K-wire complication

INTRODUCTION

Orthopaedic fixation wires has been widely used in the surgical management of fracture. Migration of the wire has been known as a complication, but migration into the chest and causing hemoptysis are rare. This is a case report of the migratory K-wire from right clavicle to trachea, causing a the false aneurysm of the thyrocervical trunk and hemoptysis. The treatment involved removal of the wire and aneurysmectomy via thoracotomy.

CASE REPORT

A 47year-old man presented with intermittent back pain for 3 years. He was diagnosed to be myalgia and received the medical treatment. In this admission, he presented with hemoptysis for 4 days. The past history of his illness was taken. He recalled that he had motorcycle accident, 10 years ago. He had undergone an orthopaedic procedure for right clavicular fracture that involved the placement of wire. The orthopaedist told him to come back for removing off the wire. But he never follow the advice and lost the follow up. Five years later, he came back again with pus at right shoulder, so the wire was removed, but there is no medical record that how many wires

which were removed.

Physical examination shows no abnormality.

Direct laryngoscope found 1.5-cm mass at posterior wall, between true vocal cord and the trachea.

Plain film shows a long piece of K-wire, overlying right upper chest and the trachea. (Figure 1)

CT scan shows tip of the K-wire, pointed to the right posterolateral portion of the trachea and there is an intraluminal non-enhancing mass in the trachea. (Figure 2)

Esophagography were performed to rule out esophageal injury. There is smooth pressure effect from mass and tip of the K-wire is point to the mass. No leakage of contrast media is demonstrated. (Figure 3)

Then he had undergone to remove wire by thoracotomy. At that operation, there's false aneurysm of thyrocervical trunk, just distal to vertebral artery origin. The patient had complete recovery and no complication after aneurysmectomy.

¹ Department of Radiology, Buddhachinnaraj Hospital, Phitsanulok, THAILAND 65000

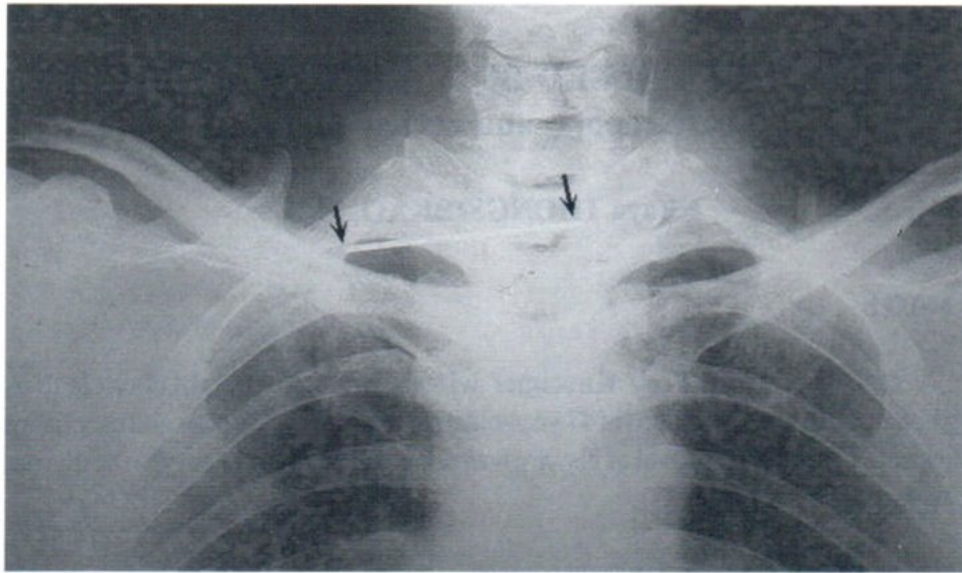


Fig.1 Metallic K-wire is seen, overlying upper chest and trachea (black arrows)

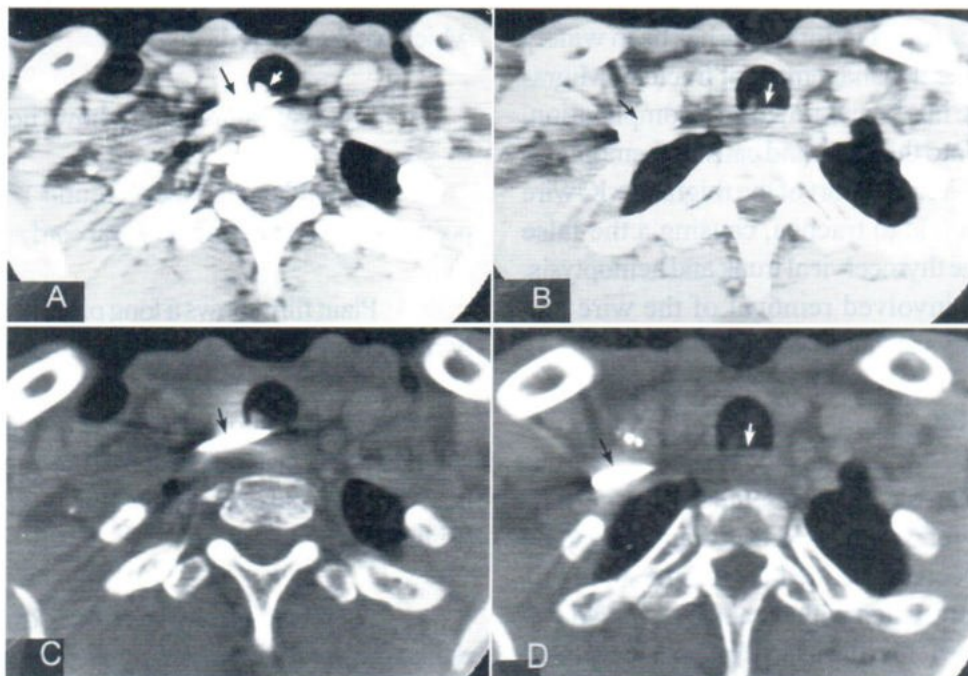


Fig. 2 Axial CT scan

- A-B** Soft tissue shadow shows a non-enhancing mass in the posterior aspect of trachea (white arrow) and a metallic K-wire (black arrow) causing artifacts to obscure the adjacent structures.
- C-D** Bone window show metallic K-wire (black arrow), pointed to the mass in the posterior aspect of the trachea (white arrow).

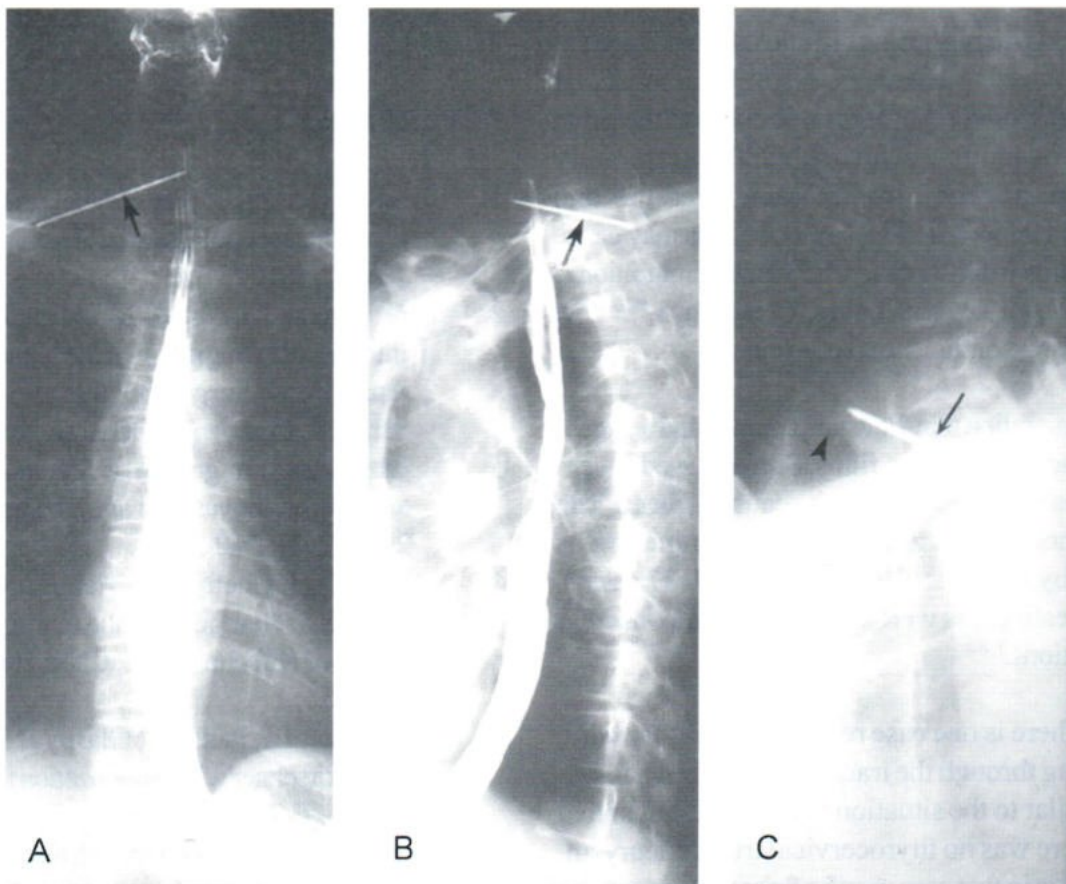


Fig. 3(A-C) Esophagogram shows no esophageal injury. Metallic K-wire is clearly seen (black arrow). Tip of K-wire is point to the posterior tracheal mass (arrow-head).

DISCUSSION

Nowadays there have been regularly using metallic fixation pin and wires in the management of fracture and dislocation. The migration of the wires and other metallic implants is a known complication to orthopaedist and surgeon, but migration of the wire to the chest is unusual.⁴⁻⁷

The first case report of migratory pin was in 1943.^{3,10} Review of the literatures, there are various unusual location of the migratory wires and pins. There have been some case reports of migratory wires from the shoulder region to the spinal canal, to the trachea, to the spleen, into pulmonary artery, into ascending aorta, into the heart, into the mediastinum, into the

lung, to the subclavian artery and travel through the pharyngeal tissue to the orbit. The various severe complications such as pericardial tamponade, arrhythmias, pericarditis, false aneurysm, aorto-innominate and aorto-pulmonary fistula, pneumothorax, hemoptysis, subclavian steal syndrome, lacerations of the subclavian artery, hemianopia, hemiplegia, paraplegia, radicular pain, dysphagia and splenic hematoma,¹⁻¹² had been reported.

The highest incidence of migration occurred when the pins and wires were used to fix anterior sterno-clavicular joint dislocations, acromioclavicular joint dislocation and fractures of clavicle.^{2-3,7} The

reason for wire migrations is unclear, but there are many proposals such as the result from muscular activity, regional resorption of bone and the great freedom of motion of the shoulder. Respiratory excursion, negative intrathoracic pressure and gravitational force, as well as electrolysis may cause the migration to the thorax.^{1,3-4,7-8} Time of migration is variable from several hours,¹² few days,⁹⁻¹⁰ few weeks,⁸ few months³⁻⁴ to many years.⁴⁻⁵

Migration may be asymptomatic and accidentally found by follow up films. Some caused severe symptoms and some may be the cause of death. The overall mortality resulting from pin migration as reported by Lyons et al has been 21% (8/37 cases). Mostly death cases were caused by cardiovascular complications.^{1,6-7}

There is one case report of migratory wire, penetrating through the trachea and caused hemoptysis, similar to the situation in this case, but in that report there was no thyrocervical trunk aneurysm. Hemoptysis in that case may be from irritation of the tracheal lining by the wire.^{2,4}

To avoid this complication by bending the distal end of wire and leaving a portion of wire out of the skin, remove the wires as soon as possible and regular follow up until the wires are removed.⁹⁻¹⁰ A record of the number of pins or wires inserted should be done to avoid leaving the one that has already migrated at the time of extraction.⁷

Radiologist should pay more attention to the case of wire fixation and the consecutive films should be follow up to detect for the wire migration.

ACKNOWLEDGEMENT

I would like to thank Professor Narong Boonyarattavej, Department of Orthopaedic surgery, Siriraj hospital, Mahidol university for his advice and comment in this paper and Dr. Piyapun Pamornsing, Department of surgery, Buddhachinnaraj hospital for

the information of this case.

REFERENCES

1. S.R.Hazelrigg,B. Staller. Migration of sternal wire into ascending aorta. *Ann Thorac Surg* 1994; 57: 1023-24
2. N. Venissac,M. Alifano,M.Dahan,J.Mouroux. Intrathoracic migration of the Kirschner pins. *Ann Thorac Surg* 2000; 69 : 1953-55
3. Sarper A,Urguden M,Dertsiz L, Demircan A. Intrathoracic migration of Steinman wire. In *teractive cardiovascular and Thoracic Surgery* 2003; 2(2): 210-1
4. Foster GT, Chetty KG, Mahutte K, Kim JB, Sasse SA. Hemoptysis due to migration of a fractured Kirschner wire. *Chest* 2001; 119(4): 1285-86
5. Goodsett JR, Pahl AC, Glaspy JN, Schapira MM. Kirschner wire embolization to the heart. *Chest* 1999; 115: 291-3
6. Lyons FA, Rocwood CA Jr. Migration of pins used in operations of the shoulder. *J Bone Joint Surg Am* 1990; 72(8): 1262-67.
7. Abdelnoor J, Mantoura J, Nahas A. Cervico-thoracic pin migration following open reduction and pinning of a clavicular fracture. *Eastern Journal of Medicine* 2000; 5(1): 26-8
8. Liu HP, Chang CH, Lin PJ, Chu JJ et al. Pulmonary artery perforation after Kirschner wire migration: *J Trauma* 1993; 34(1): 154-6
9. Bedi GS, Gill SS, Singh M, Lone GN. Intrathoracic migration of a Kirschner wire. *J Trauma* 1997; 43(5): 865-6
10. Fuster S, Palliso F, Combalia A, Sanjuan A, Garcia S. Intrathoracic migration of a Kirschner wire. *Injury* 1990; 21 (2): 124-6
11. Eaton R, Serletti J. Computerized axial tomography-A method of localizing Steinmann pin migration. A case report. *Orthopaedics* 1981; 4: 1357-60
12. Lindsey RW, Gutowski WT. The migration of a broken pin following fixation of the A-C joint. *Orthopaedics* 1986; 3: 413-6

THE STUDY OF ABSORBED DOSE DETERMINATION IN HIGH ENERGY ELECTRON AND PHOTON BEAMS USING NEW CODE OF PRACTICE IAEA-TRS 398 COMPARED WITH IAEA-TRS 277

Sivalee SURIYAPEE,¹ Tassanee LAYANGKUL,² Surat VINIJSORN,³
Siri SRIMANOROTH⁴

ABSTRACT

In Thailand, the Secondary Standard Dosimetry Laboratory (SSDL) provided the calibration factors to the hospitals all over the country for the absorbed dose determination in external beam radiotherapy using IAEA - TRS 277 protocol. The SSDL started the project of using TRS 398 protocol instead of TRS 277 protocol by providing the $N_{D,w}$ factors for the hospitals who participated in the project. Three university hospitals from ten hospitals which participated in this project were selected for analyzing the absorbed dose determined by TRS 398 compared with TRS 277. For photon beams, the measurement were performed in water phantom for 6 and 10 MV x-ray beams and Cobalt-60 gamma beams with NE 2571 0.6 cc thimble chamber. For electron beams, the cross calibration of PTW 23343 Markus chamber with NE 2571 chamber were performed to derive the $N_{D,w}$ factor for the highest electron energy. Then the dose measurement of the highest electron beams were undertaken with Markus chamber in water phantom. The results show the comparable of absorbed dose to water of photon beams determined by both TRS 398 and TRS 277 with the maximum discrepancy of 0.9%. But for electron beams, the maximum discrepancy is high up to 5%. The complicated technique of electron measurement may cause the uncertainty both in the measurement and also in the absorbed dose determination. Before the implementation of the new code of practice, studying and understanding the code of practice is necessary.

INTRODUCTION

The absorbed dose determination in external beam radiotherapy using the calibration factor in term of absorbed dose to water $N_{D,w}$ was introduced by IAEA-TRS 398¹ instead of using the calibration factor based on air kerma, N_k by IAEA-TRS 277.² The project of using the new IAEA code of practice

TRS 398 in Thailand has started by Division of Medical Device, Secondary Standard Dosimetry Laboratory (SSDL) since 2002. The aim was to introduce the hospital to be familiar and to start using the new protocol before implementation to the clinic. The hospital that participated in this project sent the

¹ Division of Radiation Oncology, Department of Radiology, Faculty of Medicine, Chulalongkorn University, Rama IV road, Bangkok, Thailand.

² Division of Radiation Oncology, Department of Radiology, Faculty of Medicine, Ramathibodi Hospital, Mahidol University, Rama VI Road, Bangkok, Thailand.

³ Division of Radiation Oncology, Department of Radiology, Faculty of Medicine, Siriraj Hospital, Mahidol University, Bangkok, Thailand.

⁴ Division of Radiation and Medical Devices, Department of Medical Sciences, Ministry of public Health, Nonthaburi, Thailand.

dosemeter to the SSDL for N_k and $N_{D,w}$ calibration factor. After the calibration factors have been provided, all hospitals were requested to make the measurement for 6 and 10 MV photon beams, Cobalt-60 gamma beams and the highest energy electron beams. The worksheets for absorbed dose determination for each type of beam were also sent to the hospitals. The SSDL gave both TRS 277 and TRS 398 worksheet and the parameters for absorbed dose determination of both protocol were needed to be filled and sent back to SSDL. There were ten hospitals participated in this project. In this study, we analyzed three university hospitals that completed all types of required radiations. The absorbed dose to water at D_{max} based on the absorbed dose to water concept $N_{D,w}$ and the air kerma concept N_k are compared.

MATERIALS AND METHODS

Three hospitals in this study comprise of King Chulalongkorn Memorial hospital, Ramathibodi

hospital and Siriraj hospital. Table 1 shows the types of the radiotherapy machines and the beams used for each hospital. Table 2 shows the types of dosimeter system used and the calibration factors for photon beams which supplied by the SSDL. For photon beams, the measurements were performed in water phantom with NE 2571 0.6 cc thimble chamber for field size of 10x10 cm. The TRS 277 recommended the measurement at the effective point which is displaced from the center of the chamber equals to 0.6 cc of the radius of the chamber. While the TRS 398 recommended the measurement at the center of the chamber. The reference depth are 5 cm for 6 MV photon beams and Cobalt-60 beams and 10 cm for 10 MV photon beams. King Chulalongkorn Memorial hospital and Siriraj hospital made the measurements by placing the chamber center at a reference depth, Ramathibodi hospital placed the chamber at the effective point of measurement at a reference depth. The absorbed dose to water at D_{max} for each protocol was calculated by the percentage depth dose at depth which the chamber was placed.

Table 1. Types of the radiotherapy machines and the beams from three university hospitals

Hospital	Machine	Beam
Chula:	Clinac 1800	6, 10 MV X-ray, 20 MeV electrons
	Theratron 80 Elite	Co-60 gamma beams
Rama:	Clinac 2100C	6, 10 MV X-ray, 20 MeV electrons
	Theratron 780C	Co-60 gamma beams
Siriraj:	Clinac 23 EX	6, 10 MV X-ray, 22 MeV electrons
	Theratron 780C	Co-60 gamma beams

Table 2. Types of chambers and dosimeters for photon beam measurements with the calibration factors that supplied by SSDL both in $N_{D,w}$ and N_k and the ratio of $N_{D,w}/N_k$.

Dosimeter	Chamber	N_k (Gy/C)	$N_{D,w}$ (Gy/C)	$N_{D,w}/N_k$
NE 2590A, SN 223	NE 2571, SN 1633	4.155×10^7	4.527×10^7	1.0895
NE 2590E, SN 360	NE 2571, SN 2289	4.170×10^7	4.556×10^7	1.0926
NE 2670A, SN 321	NE 2571, SN 3197	4.134×10^7	4.522×10^7	1.0938

For electron beams, the cross calibration of PTW 23343 Markus chamber with 0.6 cc thimble chamber were performed to determine $N_{D,w}$ of the highest energy of electron beams (20-22 MeV). The beam size was 10x10 cm. For a new IAEA protocol, the chamber was placed at the reference depth (Z_{ref}) which equals to $0.6 R_{50} - 0.1$ cm for plane-parallel chamber and at $Z_{ref} + 0.5$ radius of chamber for 0.6 cc chamber while for TRS 277 protocol the chamber was placed at the depth of maximum dose. When the $N_{D,w}$ was determined, the calibration of the highest energy electron beams was performed. The measurement was undertaken for both protocols at maximum field size, which two hospitals used 25x25 cm and the other one used 15x15 cm. The position of the chamber was at the depth as stated above.

The absorbed dose to water was calculated by following equations:

$$\text{TRS 277 } D_{w,Q} = M_Q N_{D,air} (S_{w,air})_Q p_Q \quad \text{—————1}$$

$$\text{TRS 398 } D_{w,Q} = M_Q N_{D,w,Q0} k_{Q,Q0} \quad \text{—————2}$$

M_Q is the reading of dosimeter corrected for recombination and environment condition.

$N_{D,air}$ is the absorbed dose to air chamber factor base on air kerma, $(S_{w,air})_Q$ is the stopping power ratio water to air at the user's quality at the point of interest and p_Q is the perturbation correction factor. $N_{D,w,Q0}$ is the calibration factor in term of absorbed dose to water at a reference beam quality Q_0 and

$k_{Q,Q0}$ is a chamber specific factor which corrects for differences between the reference beam quality Q_0 and the actual beam quality Q .

RESULTS

The ratio of the calibration factors of N_k and $N_{D,w}$ determined by the SSDL which are shown in table 2 for three hospitals are in the same range. The variation between the chambers is less than 1%. Table 3 shows the comparison of the absorbed dose to water at D_{max} between TRS 398 and TRS 277 for 6 and 10 MV together with the beam parameters used for absorbed dose determination, while Table 4 shows the comparison of the absorbed dose to water at D_{max} between TRS 398 and TRS 277 for Cobalt-60 gamma rays and also the beam parameters. King Chulalongkorn Memorial and Siriraj hospital set the center of the beams at the center of the chamber (TRS 398) while Ramathibodi hospital set the measurement point at effective points (TRS 277) which are shifted from the center of chamber toward the surface. All the hospital made the measurement only one depth and used this data to determine the absorbed dose both in TRS 277 and TRS 398. The percentage depth dose at depth were used to calculate the absorbed dose to water at D_{max} , the depth and percentage depth dose for each protocol are also shown in Table 3 and Table 4. The ratio of the absorbed dose to water at D_{max} determined by TRS 398 and TRS 277 for photon beams are mostly higher than TRS 277. The maximum discrepancy is 0.9%

for all energy and beam studied.

For electron beams, Table 5 shows the types of chamber and the cross calibration factor of electron beams. Table 6 shows the comparison of

the absorbed dose to water at D_{max} determined by TRS 398 and TRS 277 for the large field size and high energy electron beams. The discrepancy between TRS 277 and TRS 398 protocol is as high as 5% for one of the three hospitals.

Table 3. Comparison of the absorbed dose to water at D_{max} (cGy/mu) for TRS 398 and TRS 277 of 6 and 10 MV x-ray beams, 10x10 cm, 100 cm SSD. The absorbed doses at the depth of measurement are also shown, with the parameters used for dose determinations.

Unit	Energy (MV)	TRS 277					TRS 398				TRS 398/277
		TPR _{20,10}	Depth (cm)	%DD (%)	D_{ref}^*	D_{max}^{**}	Depth (cm)	%DD (%)	D_{ref}^*	D_{max}^{**}	
Clinac1800	6	0.6770	4.80	87.40	0.895	1.024	5.0	86.60	0.885	1.022	0.998
Clinac 2100C	6	0.6725	5.00	87.08	0.856	0.983	5.2	86.27	0.850	0.985	1.002
Clinac 23EX	6	0.6720	4.80	86.58	0.875	1.011	5.0	85.30	0.870	1.020	1.009
Clinac 1800	10	0.7380	9.80	74.50	0.753	1.011	10.0	73.70	0.748	1.015	1.004
Clinac 2100C	10	0.7353	10.00	73.65	0.728	0.988	10.2	73.05	0.725	0.993	1.005
Clinac 23EX	10	0.7381	9.80	73.68	0.742	1.007	10.0	73.00	0.739	1.012	1.005

* D_{ref} = Absorbed dose in cGy/mu at the reference depth of measurements

** D_{max} = Absorbed dose in cGy/mu at the depth of maximum dose

Table 4. Comparison of the absorbed dose to water at D_{max} (cGy/mu) for TRS 398 and TRS 277 of Co-60 gamma beams, 10x10 cm, 100 cm SSD.

Unit	Energy (MeV)	TRS 277				TRS 398				TRS 398/277
		Depth (cm)	%DD (%)	D_{ref}	D_{max}	Depth (cm)	%DD (%)	D_{ref}	D_{max}	
Co-60 Elite	1.25	4.80	79.50	166.40	209.31	5.0	78.25	164.12	209.74	1.002
Co-60 780C	1.25	5.00	78.80	85.73	108.79	5.2	77.82	84.78	108.94	1.001
Co-60 780C	1.25	4.80	79.17	169.70	214.35	5.0	78.40	168.27	214.63	1.001

Table 5. Type of chambers and calibration factors for electron measurement.

Dosemeter	Chamber	N_k (Gy/C)	$N_{D,W(cross)}$ (Gy/C)
NE 2590A, SN 223	PTW 23343, SN 1042	4.708×10^8	4.628×10^8
NE 2590E, SN 360	PTW 23343, SN 2380	4.968×10^8	4.690×10^8
NE 2670A, SN 321	PTW 23343, SN 3485	5.044×10^8	5.232×10^8

Table 6. Comparison of the absorbed dose to water at D_{max} (cGy/mu) for TRS 398 and TRS 277 of electron beams, 100 cm SSD

Unit	Energy (MeV)	Field size (cm)	TRS 277		TRS 398				TRS 398/277
			d_{max} (cm)	D_{max} (cGy/mu)	Z_{ref} (cm)	%DD (%)	D_{ref} (cGy/mu)	D_{max} (cGy/mu)	
Clinac 1800	20	25x25	2.00	0.848	5.00	96.0	0.8120	0.846	0.997
Clinac 2100C	20	25x25	2.80	0.90116	5.10	94.5	0.8109	0.858	0.952
Clinac 23EX	22	15x15	2.64	1.01020	5.19	95.5	0.9774	1.023	1.013

DISCUSSION AND CONCLUSION

This paper presents results of measurements of absorbed dose to water in high energy photon and electron beams following the recommendations of TRS 398 and TRS 277. The variation of $N_{D,w} / N_k$ for three hospitals is less than 1%. The absorbed dose for photon beams show the agreement for both protocol with the maximum discrepancy of 0.9%. Most of the results show the higher dose for TRS 398 than TRS 277. For electron beams, the procedure may be complicated with many changes for measurement and for the absorbed dose determination. So the discrepancy is going up to 5%. Huq³ reported the

results for photon beams using TRS 398 are about 1% larger than those obtain with TRS 277 for most commonly used clinical beam qualities. For electron beam quality range of 2.27-8.13 cm, a maximum discrepancy of about 2% are observed between TRS 398 and TRS 277. Our study for photon beams are comparable to Huq's report but not for electrons. However, these measurements are the experimental study and the implementation of TRS 398 in the clinical for all institutes in the country will be continued with the assistance of SSDL and IAEA in term of expert and documents.

REFERENCES

1. Absorbed dose determination in external beam radiotherapy. An International Code of Practice for Dosimetry Based on Standards of Absorbed dose to water. IAEA TRS 398, Vienna 2000.
2. Absorbed dose determination in photon and electron beams. An International Code of Practice IAEA TRS-277, Vienna 1987.
3. Huq MS. Intercomparison of absorbed dose to water and air kerma based dosimetry protocols for photon and electron beams. Standards and Codes of Practice in Medical Radiation Dosimetry. Proceedings of an International Symposium, Vienna, 25-28 November 2002. Vol 1, IAEA - CN - 96, International Atomic Energy Agency, Vienna, 2003.

GASTRIC OUTLET OBSTRUCTION DURING BONE SCAN.

Dr. M.A. Taher

ABSTRACT

A female patient of 40 years was diagnosed to have gastric outlet obstruction during radionuclide bone scintigraphy (Fig.1)

INTRODUCTION

Noninvasive measurement of gastric accommodation and emptying with radionuclide technetium 99 metastable (^{99m}Tc) is feasible.¹ At present, a barostat study is the gold standard, but it is invasive and possibly induces artifacts as a result of positive intraluminal balloon pressure.

CASE REPORT

A female patient of 40 years came for whole body bone scan after left-sided mastectomy due to duct cell carcinoma and desmoplasia. Intravenous injection of 20 milli-Curies ^{99m}Tc MDP (methylene diphosphonate) was given. Blood pool images under Siemens gamma camera were normal, but static views after 3.5 hours showed only non-osseous uptakes in right breast nodule and unusually distended stomach. Ultrasound scan by sonoline SL-2 showed a 9.9 mm hyperechoic nodule in right breast, pockets of small ascites, slow gastric emptying and lower part of esophagus was inflamed.² The patient vomitted during gamma camera scan (static view). The patient complained of anorexia and nausea, but never vomitted before.

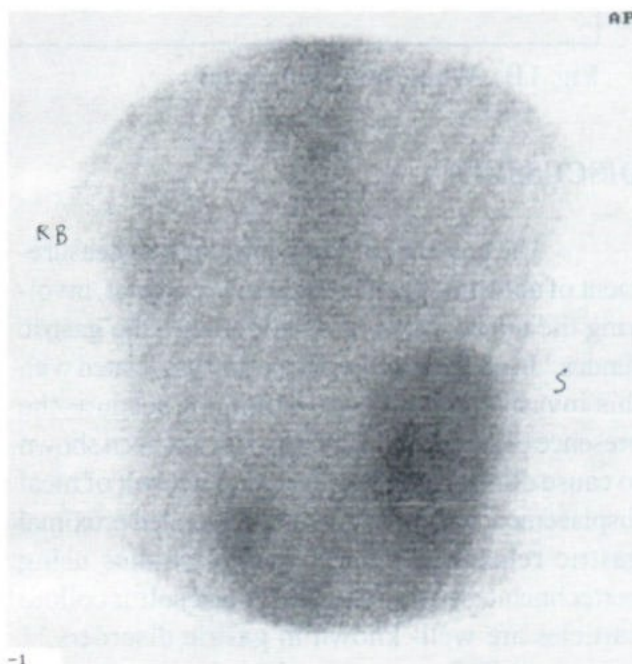


Fig. 1A ^{99m}Tc MDP uptake in stomach (S) and right breast (RB)

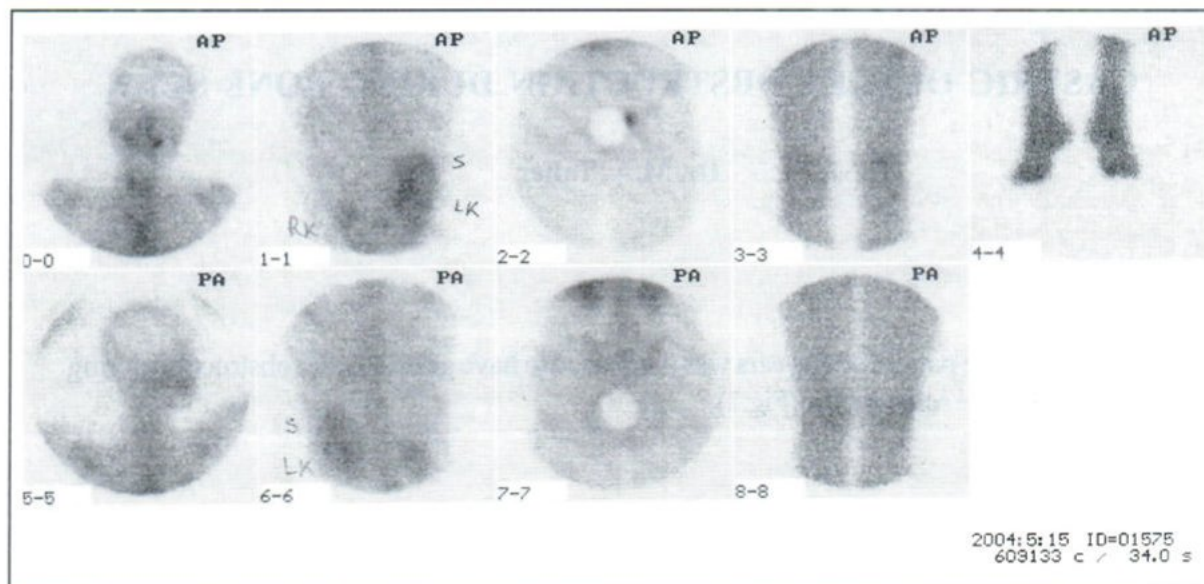


Fig. 1B Whole body bone scan

DISCUSSION

The current gold standard for the measurement of accommodation is the gastric barostat, involving the introduction of a balloon into the gastric fundus.³ In addition to the discomfort associated with this invasive and time-consuming procedure, the presence of a balloon in the stomach has been shown to cause dilatation of the antrum as a result of meal displacement and induction of exaggerated proximal gastric relaxation.⁴ Radionuclide studies using pertechnetate, sucralfate, DTPA and sulfur colloid particles are well-known in gastric disorders,^{5,6} however, MDP was not used for this purpose yet, although non-osseous uptake of MDP during three-phases bone scan is a recognized fact.⁷ The stomach uptake must be distinguished from splenic or renal accumulation.⁸ The mechanism for localization of bone-scanning agents in noncalcified soft tissue, particularly damaged muscle, may be related to movement of calcium from plasma into damaged muscle cells through abnormally permeable sarcolemma.⁹ Other possible mechanisms of soft-tissue uptake include binding to immature collagen and atypical binding of the Tc-99m phosphate to phosphatase enzymes.^{10,11}

REFERENCES

1. Bennink RJ, van den Elzen BD, Kuiken SD, Boeckxstaens GE. Noninvasive measurement of gastric accommodation by means of pertechnetate SPECT: Limiting radiation dose without losing imaging quality. *J Nucl Med* 2004; 45:147-152.
2. Alam MS, Rahman MM, Ahmed AU, Hossain MA, Mohammad J, Mazumder S, Ahmed MS, Ferdousi MA. Evaluation of oesophageal varices with transabdominal ultrasound. *Asian Oceanian J Radiol* 2003; 8: 37-41.
3. Azpiroz F, Malagelada JR. Gastric tone measured by an electronic barostat in health and postsurgical gastroparesis *Gastroenterology* 1987; 92: 934-943.
4. Mundt MW, Hausken T, Samsom M. Effect of intragastric barostat bag on proximal and distal gastric accommodation in response to liquid meal. *Am J Physiol Gastrointest Liver Physiol*. 2002; 283: G681-G686.

5. Puttemans NAM, Andre PP, Jamsin SAMJ, Balikhhan DPH, Lustman F. Detection of gastroduodenal ulcers using technetium - 99m -labeled sucralfate. In Biersack HJ, Cox PH (eds.) *Nuclear Medicine in Gastroenterology* 139-151, 1991 Kluwer, Dordrecht, the Netherlands.
6. Bares R, Buell U. Gastroesophageal and biliary reflux. In Biersack HJ, Cox PH (eds.) *ibid.*
7. Taher MA. Non-osseous uptakes of Tc-99m phosphonate during three phases bone scanning. *ASEAN J Radiol* 2003; IX; 139-142.
8. Wilson MA, Pollack MJ. Gastric visualization and image quality in radionuclide bone scanning: concise communication. *J Nucl Med* 1981; 22: 518-521.
9. Siegel BA, Engel WK, Derrer EC. Localization of technetium 99m diphosphonate in acutely injured muscle. Relationship to muscle calcium deposition. *Neurology* 1977; 27:230.
10. Jones AC, Francis MD, Davis MA. Bone scanning: Radionuclide reaction mechanisms. *Semin Nucl Med* 1976; 6: 3.
11. Rosenthal L, Kaye M. Observations in the mechanism of 99m Tc- labeled phosphate complex uptake in metabolic bone disease. *Semin Nucl Med* 1976; 6: 59.

NUCLEAR ONCOLOGY

Dr. M.A. Taher

Various radionuclides or isotopes are used in the imaging and treatment of cancers in different organs of human body (Table 1).

TABLE 1 Radionuclides used in cancer

Organ	Isotope	Chemical form	Time of scan
Thyroid	I-131	Nal	24-72h after oral dose
Liver	Tc-99m	Colloid	Immediate post-injection (i.v.)
	I-131 /Re- 188	poppyseed oil (Lipiodol)	
Bone	Tc-99m	Methylene Diphosphonate (MDP)	Three phase study: 0-3 h after i.v.inj.
Colon and Rectum	Tc-99m	Antibody	2-5h post-inj i.v.
Kidney	Tc-99m	Diethylene triamine penta acetic acid (DTPA)	0-3h post-inj i.v.
		Dimercapto-Succinic acid (DMSA)	
Lymph-node	Tc-99m	Colloid	0-1h post-inj subcutaneously
Neuro-endocrine tumor	I-131	Meta-iodo-benzyl-guanidine(MIBG)	2-5 days post-inj.
	I-123		
Malignant ascites/pleural effusion	P-123	Colloidal chromic phosphate	

THYROID

The great Arab physician Abul Quasim was the first who used thyroid aspirates to differentiate various types of goitres (1013-1107 A.D.)¹ Since 1938, radioiodine is being used in the diagnosis and treatment of thyroid diseases. It is used for assessing functional status of nodular goitre. In a biopsy-proven papillary/follicular carcinoma of thyroid gland post-thyroidectomy remnant ablation is done by a 29 milli-Curies dose of ¹³¹I and a whole-body gamma-scan is done to detect any occult metastasis. Follow -up

scans are done after 3-6 months intervals with thyrotropin stimulation (avoiding thyroxine for six weeks and tri-iodothyronine for three weeks).¹⁸ ¹⁸F fluorodeoxyglucose (FDG) is used in scanning thyroid metastases in presence of thyroxine feeding. Positron emission tomography (PET) cameras dedicated to oncology, or single photon emission computed tomography (SPECT) cameras with systems of positron coincidence detection are becoming reference techniques.² However, radio-

fluorine is not yet available in Bangladesh. "Hot" nodules that take up radioiodine in excess of the surrounding thyroid have a low probability of malignancy, estimated at 1% to 4%.³ Warm nodules, having uptake about the same as that of the surrounding thyroid, are usually adenomas but have about a 10% chance of being malignant.⁴ Cold nodules have about a 10% to 25% chance of malignancy and require aspiration biopsy; nevertheless, the great majority of cold nodules are benign. Human TSH (thyroid stimulating hormone or thyrotropin), commercially known as thyrogen is being used in some countries to search thyroid metastases quickly, but its clinical utility and cost-effectiveness is not beyond doubt. Whole-body radioiodine scans for detection of residual and metastatic disease before ablation or treatment can be done with a diagnostic 2mCi dose of ¹³¹I, although generally all that is identified is residual thyroid tissue and this low dose of ¹³¹I may reduce uptake of the subsequent ablative therapy dose, in a process known as stunning.⁵ When substantial locoregional disease is detected, or excessive thyroid remnants are identified by scanning (radioiodine uptake >5-10%), additional surgery before radioiodine administration should be strongly considered. A scan is often done several days after administration of the therapeutic radioiodine dose. This post-treatment scan has a greater sensitivity to detect metastatic disease than the pre-ablation diagnostic scan, because sensitivity relates directly to the amount of radioiodine given.^{6,7} By providing evidence of metastatic disease, post-treatment scans can help physicians to decide on the intensity of future diagnostic procedures and treatments.⁷

LYMPH NODE

Lymphoscintigraphy and sentinel lymphnode mapping by surgical gamma probe are very useful procedures in the patients with breast cancer. Sentinel lymph node (SLN) is the first lymph node encountered by lymphatic vessels draining a tumour. The SLN will most likely be the first to be affected by metastasis, and a negative SLN makes it highly

unlikely that other nodes are affected. In breast cancer surgery, axillary node dissection is performed to stage the axilla and does not improve prognosis of the patients. It can also lead to significant morbidity. As 70% of patients are free from metastases, SLN biopsy might replace complete axillary dissection to stage the axilla in clinically no node palpable patients. SLN biopsy can also increase accuracy of histopathologic staging of the axilla by focusing on the SLN. The practice of SLN biopsy requires collaboration among surgical oncologists, nuclear medicine physicians, histopathologists and medical physicists. Nuclear Medicine physicians are responsible for administration of radiopharmaceutical and performing lymphoscintigraphy (SLN imaging). ^{99m}Tc labelled colloids with majority of the particles in the 100-nm to 200-nm size range provide the best results for SLN biopsy in breast cancer. There are four variables in the administration of radiocolloids: site of injection, volume of the injectate, radioactivity injected and the timing of the injection relative to the surgery. 0.5 to 5 ml of radiocolloids with radioactivity varying from 0.5 to 10 mCi have been used. The injection can be made into the tumour, the parenchyma surrounding the tumour, the skin overlying the tumour or the subareolar region of the breast.²⁶⁻²⁸

KIDNEYS

Both Wilms tumor and renal adenocarcinoma may show varying vascular patterns in dynamic renal scan, followed by irregularly spheric voids seen on static scintigrams. An unusually high vascular perfusion pattern suggests arteriovenous malformation (AVM) or the rare angiolipoleiomyoma (ALM) rather than malignant neoplasm.²⁹ Radionuclide renogram provides accurate informations regarding individual kidney functions and may help to monitor therapy of various cancers if needed.

NEURO-ENDOCRINE TUMORS

Adrenal medulla and neuro-endocrine tumors can be imaged by MIBG and also treated by MIBG

labelled by ^{131}I . In 1987, Beierwaltes et al¹⁴ gave C-labelled precursors of epinephrine to dogs and sacrificed the dogs at 6 hr. Then they developed norepinephrine structured analogs.³⁰ MIBG may concentrate diagnostically ^{123}I or ^{131}I and therapeutically ^{131}I in all tumors with neurosecretory granules, e.g. medullary thyroid carcinoma, carcinoid, small cell carcinoma of the lung, Merkel cell carcinoma of the skin, gastrinomas, and insulinomas.¹²⁵ MIBG is being investigated to treat neuroblastomas, the cells of which may be interspersed with normal bone marrow cells.¹²⁵ ^{125}I is an ultra-short-range auger electron emitter, with a range of 10 nm and is localized intracellularly within the nucleus.³¹

REFERENCES

1. Muhsin AUM. Cytologic diagnosis: a review. Bangladesh Med Res Counc Bull 2002; 28 (2): 82-86.
2. Chatal J-F. Recent advances in immunoscintigraphy and radioimmunotherapy. Kaku Igaku (Jpn J Nucl Med) 1997; 34:729-30.
3. Hopkins CR, Reading CC: Thyroid and parathyroid imaging. Semin Ultrasound CT MRI 1995; 16: 279-295.
4. Price DC: Radioisotopic evaluation of the thyroid and parathyroids. Radiol Clin North Am 1993; 31: 991-1015.
5. Sherman SI Thyroid carcinoma Lancet 2003; 361:501-11.
6. Sherman SI, Tielens ET, Sostrs S, Wharam MD Jr, Ladenson PW Clinical utility of posttreatment radioiodine scans in the management of patients with thyroid carcinoma. J Clin Endocrinol Metab 1994; 78: 629-34.
7. Reynolds JC. Percent ^{131}I uptake and post-therapy ^{131}I scans: their role in the management of thyroid cancer. Thyroid 1997; 7: 281-84.
8. Fleming, J S Ackery, D.M. Walmsley, B H, Karran, S J Scintigraphic estimation of arterial and portal blood supplies to the liver. Journal of Nuclear Medicine, 1983; 24: 1108-1113.
9. Leveson, S. H. Wiggins, P A Nasiru T A Giles G R, Robinson P J Improving the detection of hepatic metastases by the use of dynamic flow scintigraphy. British Journal of Cancer, 1983; 47: 719-721.
10. Borzutzky C A & Turbiner EH. The predictive value of hepatic artery perfusion scintigraphy. Journal of Nuclear Medicine. 1985; 26: 1153-1156.
11. Ziessman HA, Wahl RL, Juni JE, Gyves JE, Ensminger WD, Thrall JH, Keyes JW et al. The utility of SPECT for 99m Tc-MAA hepatic arterial perfusion scintigraphy. American Journal of Roentgenolgy, 1985; 145: 747-751.
12. Buscombe JR. Interventional nuclear medicine in hepatocellular carcinoma and other tumors Nucl Med Commun 2002; 23 (9): 837-41.
13. Gnanasegaran G, Buscombe JR. Neuroendocrine tumors-Part two. The role of nuclear medicine in treating Neuroendocrine tumors. World J Nucl Med 2003; 2: 314-323.
14. Roul J L, Guyander D, Bretagne J F, et al. Prospective randomized trial of chemoembolisation versus intra-arterial iodine-131 lipiodol in inoperable hepatocellular carcinoma. Hepatol 1997; 26: 1156-1161.
15. Anonymous. New drugs. Aust Prescr 2003; 26: 68.
16. Lechner P, Lind P, Goldenberg DM. Can postoperative surveillance with serial CEA immunoscintigraphy detect resectable rectal cancer recurrence and potentially improve tumor-free survival? J Am Coll Surg 2000; 191: 511-8.

17. Willkomm P, Bangard M, Decker P, Grunwald F, Biersack HJ. FDG PET and immunoscintigraphy with ^{99m}Tc-labeled antibody fragments for detection of the recurrence of colorectal carcinoma. *J Nucl Med* 2000; 41: 1657-63.
18. Libutti SK, Alexander HR, Choyke P, Bartlett DL, Bacharach SL, Whatley M, et al. A prospective study of 2-fluoro-2-deoxy-D-glucose/positron emission tomography scan, ^{99m}Tc-labeled arcitumomab (CEA scan), and blind second-look laparotomy for detecting colon cancer recurrence in patients with increasing carcinoembryonic antigen levels. *Ann Surg Oncol* 2001; 8: 779-86.
19. Goin JE, Dancey JE, Hermann GA, Sickles CJ, Roberts CA, Macdonald JS. Treatment of unresectable metastatic colorectal carcinoma to the liver with Intrahepatic Y-90 microspheres: dose-ranging study. *World J Nucl Med* 2003; 2 216-225.
20. Taher MA. Non-osseous uptake of Tc-99m phosphonate during three phase bone scan. *ASEAN J Radiol* 2003; IX: 83-84.
21. Mckillop J H. Bone Scanning In Metastatic Disease. In Fogelman I (editor): *Bone Scanning in Clinical Practice* London: Springer- Verlag, 1987.
22. Borak J. Relationship between the clinical and roentgenological findings in bone metastases. *Surg Gynecol Obstet* 1942; 75: 599-604.
23. Clain A. Secondary malignant disease of bone. *Br J Cancer* 1965; 19: 15-29
24. Shackman R, Harrison CV. Occult bone metastases. *Br J Surg* 1947; 35:385-389.
25. Aoki J, Watanabe H, Shinozala T, Tokunaga M, Inoue T, Endo K. FDG-PET in differential diagnosis and grading of chondrosarcomas. *J comput Assist Tomogr* 1999 Jul-Aug; 23(4): 603-8.
26. Ho WY, Sentinel Node Imaging. Hong Kong College of Radiologists 10th Annual Scientific Meeting; 19th & 20th October 2002.
27. Ege GN. Internal mammary lympho scintigraphy the rationale, technique, Interpretation, and clinical application. *Radiology* 1976; 118:101.
28. Abdel-Dayem HM, Siraj QH, Collier BD. Lymphoscintigraphy. In Maissey MN, Britton KE, Collier BD (eds): *Clinical Nuclear Medicine*, 3rd ed. pp. 541-552, Chapman & Hall, 1998, London.
29. Tauxe WN, Dubovsky EV. The genitourinary system. In Harbert J, Da Rocha AFG (editors): *Textbook of Nuclear Medicine* vol. II 1984, Philadelphia, Lea & Febiger, pp.481-521.
30. Beierwaltes WH, Sisson J C, Shapiro B. Radionuclide therapy of adrenocortical and medullary tumors. In Spencer R P, Seever R H, Friedman A M (eds.): *Radionuclides in therapy*. 1987 C R C Press, Florida, pp. 47-62.
31. Wilson M A, Hammes R. J. Radiopharmaceuticals. In Wilson M A (ed): *Textbook of Nuclear Medicine*, 1998, Lippincott-Raven, Philadelphia, pp. 385-413.

MATERNAL SCREENING OF THYROID FUNCTION

Dr. M.A. Taher

Pregnant women comprise the most vulnerable population group with respect to iodine deficiency, because of its causative link with cretinism, an irreversible defect resulting from severe iodine deficiency in utero. For this reason, the elimination of cretinism is one of the most important aims and monitored indices of success of community iodine supplementation programs.¹

Iodine deficiency in young children can compromise their mental development. Two studies in Bolivia and Bangladesh did not show any effect, while in two in Malawi and Benin did. It may well be that the iodine deficiency was less severe in the populations in which no effect was found compared with those in which it was.²⁻⁵

The fetus cannot make T_4 (thyroxine) in the first half of pregnancy when neuron proliferation and migration are taking place in the brain. Pop et al correlated maternal T_4 levels during 12 weeks of pregnancy with impaired infant psychomotor performance at 10 months.⁶

Azizi et al published a study on 14 children who had a transient increase in TSH (thyroid stimulating hormone or thyrotropin) and were completely normal after the 3rd month of life, and then between 4 and 6 years of age they had a much lower I.Q. (intelligence quotient) than normal children.¹

Transiently elevated TSH (or TSH surge) was found during the first 24th year of life is considered to be entirely physiological. It is at least partly due to the cooling of the neonate immediately after birth and to the cutting of the cord. This is why we have two kinds of normal levels. If the blood sample is collected right after birth or from the cord, the cut off point is about 20 mU/L., however, if you take it as a usual screening test 3 days after birth, the cutoff point will be about

5mU/L.

In conditions of mild iodine deficiency, serum free T_4 slightly decreases during gestation, while in iodine sufficiency there is only a slight (15%) decrease by the end of gestation. In mild iodine deficiency, serum TSH and thyroglobulin are still higher in neonates than in their mothers. The frequency distribution of neonatal TSH on day 5, at the time of systematic screening for congenital hypothyroidism is shifted towards elevated values. In moderate iodine deficiency, the frequency of a neonatal TSH above 20-25, mU/L blood that is above cutoff point used for recalling neonates due to suspicion of congenital hypothyroidism in programs of systematic screening for congenital hypothyroidism, is increased. The hypersensitivity of neonates to iodine deficiency is explained by their very small intrathyroidal iodine pool, which requires increased TSH stimulation and a fast turnover rate in order to maintain a normal secretion of thyroid hormones.⁸

In mild iodine deficiency, preterm infants have low total and free T_4 elevated TSH and exaggerated TSH response to TRH. This picture of primary subclinical hypothyroidism is in contrast with the picture of tertiary hypothyroidism evidenced in preterm infants in iodine replete areas, characterized by the fact that TSH remains normal in spite of low free T_4 .

In humans, T_4 is already found in the first trimester coelomic fluid from the 6th week of gestational age, a long time before the onset of fetal thyroid function, which occurs at the 24th week of gestation. The number of T_3 (triiodothyronine) receptors and the amount of T_3 bound to the receptors in the whole brain increase about 10-fold between 10 and 18 weeks, also before the onset of fetal thyroid function. At term, about 20-50% of cord serum T_4 is still of maternal origin. Maternal screening of thyroid function should be considered seriously as a part of routine antenatal check up.

REFERENCES

1. Allen L, Gillespie S. What works? A review of the efficacy and effectiveness of nutrition interventions. UN ACC/SCN Nutrition policy paper No. 19. New York, UN Administrative Committee on Coordination, 2001.
2. Bautista A, Barker PA, Dunn JT, Sanchez M, Kaiser DL. The effects of oral iodized oil on intelligence, thyroid status and somatic growth in school-age children from an area of endemic goitre. *Am J Clin Nutr* 1982; 35:127-134.
3. Huda SN, Grantham-mcGregor S, Tomkins A. Cognitive and motor function of iodine-deficient but euthyroid children in Bangladesh do not benefit from iodized poppyseed oil (Lipiodol) *J Nutr* 2001; 131:72-77.
4. Shrestha RM. Effect of iodine and iron supplementation on physical, psychomotor and mental development in primary school children in Malawi; Ph D thesis Wageningen Agricyltural University, 1994.
5. Van den Briel T, West CE, Bleichrodt N, van der Vijer FJR, Hautvast JGAJ, Ategbo EA. Improved iodine status is associated with improved mental performance of school children in Benin. *Am J Clin Nutr* 2000; 72: 1179-1185.
6. Pop VJ, Kuijpers JL, Van Baar AL, et al. Low maternal free thyroxine concentrations during early pregnancy are associated with impaired psychomotor development in infancy. *Clin Endocrinol* 1990; 50:149-155.
7. Azizi F, Khoshnati M, Bahrainian M, Hedayati M: Thyroid function and intellectual development of infants nursed by mothers taking methimazole. *J Clin Endocrinol Metab* 2000; 85: 3233-3238.
8. Delange FM. Iodine deficiency disorders in mothers and infants. In Delange FM, West KP Jr. (eds.) micronutrient Deficiencies in the First Months of life, Nestle Nutrition workshop series pediatric programs Vol. 52. pp. 89-102, Nestec Ltd. Vevey/S. Karger AG, Basel, 2003.

URETEROPELVIC JUNCTION OBSTRUCTION (UPJO) PRESENTED AS HEMATURIA.

Dr. M.A.Taher

ABSTRACT

A boy of 7 years presented with hematuria following a trivial trauma (fall on floor). On clinical examination, a small mass was palpable in the left loin, which was correlated to be the hydronephrotic left kidney (7x11cm in size) on ultrasonography (USG). Radionuclide renogram under computerized gamma camera (Siemens, Germany) using Tc99 DTPA showed normally functioning right kidney and left renal obstruction (Fig.1). Pyeloplasty was advised.

KEY WORDS: Kidney, ultrasonography, and renogram.

INTRODUCTION

Congenital narrowing at the junction of the ureter and the renal pelvis is a common developmental variant that may impede the flow of urine, causing distention of the renal pelvis as well as the major and minor calyces (hydronephrosis). In many

cases, it is difficult to differentiate between this harmless anomaly and significant, pathologic urinary tract obstruction. Congenital ureteropelvic junction (UPJ) obstruction is suggested if calyceal dilation is minimal, kidney size is normal, and renal parenchy-

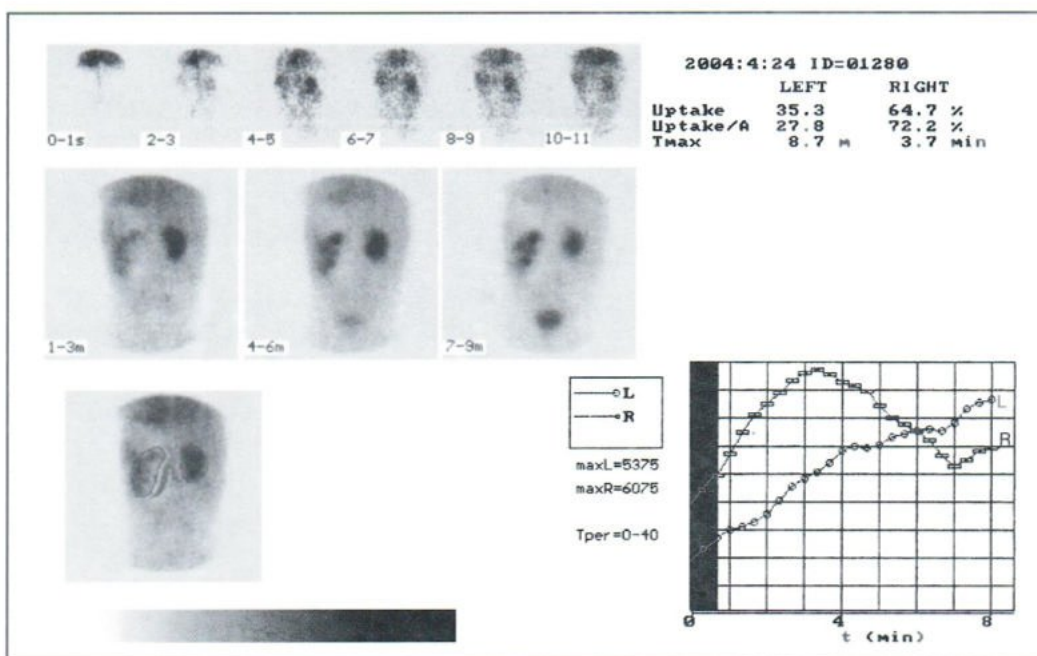


Fig 1 Left renal obstruction (DTPA Renogram)

mal thickness is normal. Moderate or severe urinary tract distention and parenchymal thinning suggest significant obstructive uropathy and are not features of innocuous UPJ narrowing.¹ Ultrasound cannot assess renal function.² Individual kidney function is important for surgical planning and can be determined by renal rediouclide scans.³

DISCUSSION

Sonography of UPJ obstruction shows a large cystic mass within the kidney. There are multiple hypoechoic cystic spaces, with the largest being medial in location and representing the dilated renal pelvis. The cysts intercommunicate and infundibulae and calyces as well as renal parenchyma are identified. IVU shows delayed excretion of contrast medium, which is diluted by retained urine within the large renal pelvis. Renogram with technitium 99 metastable diethylene triamine pentaacetic acid (Tc99m DTPA) shows a photon-deficient area due to the dilated renal collecting system; there is central

migration of isotope into the renal pelvis on delayed images. If renal function is markedly decreased, renogram will be helpful in identifying the amount of functioning renal parenchyma.⁴

REFERENCES

1. Zwiebel WJ, Normal variants and developmental anomalies of the urinary tract. In Zwiebel WJ, Sohaey R. Introduction to ultrasound. 1998 W.B. Saunders Co. Philadelphia, pp. 176-185.
2. Palmer PES (ed.). Manual of diagnostic ultrasound 2002 WHO&WFUMB.
3. Kleiner B, Callen PW, filly RA. Sonographic analysis of the fetus with ureteropelvic junction obstruction. AJR 148: 359-363, 1987.
4. Kirks DR, Laurin S. Pediatric radiology. In the NICER Centennial Global Textbook of Radiology, 1995,Oslo, pp.533-626.

ULTRASOUND IN CHRONIC ECTOPIC PREGNANCY

Dr. M.A. Taher

Chronic ectopic pregnancy is an uncommon form of tubal pregnancy with atypical pain and minimal symptoms in which there is a gradual disintegration of the tubal wall with slow and/or repeated episodes of hemorrhage leading to the formation of a pelvic mass.¹ The incidence of chronic ectopic pregnancy is 20.3% of all ectopic pregnancies.² Some patients may not give any history of amenorrhea,³ an unmarried girl denies sexual activity due to moral issues and social stigmal,⁴ but fluid collections are seen in hepatorenal space and cul-de-sac (Pouch of Douglas).

The incidence of ectopic pregnancy has been rising over the past several decades.⁵ Most current algorithms for the evaluation of the ectopic pregnancy include the use of ultrasound and Doppler flow studies with quantitative beta human chorionic gonadotropin (hCG) as needed. With the need to incorporate ultrasound into the standard evaluation of the symptomatic first-trimester patient with bleeding or pain, pelvic ultrasound for intrauterine pregnancy has become a natural application in emergency ultrasound. The presence of an intrauterine pregnancy decreases the risk of a concurrent ectopic pregnancy to 1 in 30000 for a low-risk patient and 1 in 5000 for a high-risk patient.⁶ In some ectopic pregnancies, the echogenic ring may look like the ovarian corpus luteum cyst.⁷ Although the number of ectopic pregnancies has increased, the mortality from ectopic pregnancies has decreased 90% since 1979. In 1978, Maklad and Wright⁸ wrote the first report of B-mode gray scale ultrasonography for ectopic pregnancy evaluation. Cacciatore et al⁹ found that a gestational sac was always seen by the time the β -hCG level reached 1000 IU (second International Preparation Standard), and a yolk sac should always be seen by the time the mean sac diameter (MSD) reaches 10 mm (many authorities use 8 mm as the current cutoff) on transvaginal ultrasonography.

A chronic ectopic pregnancy is manifested sonographically by an extrauterine complex mass in the adnexae and cul-de sac along with a slightly enlarged uterus with no evidence of an intrauterine pregnancy. The adnexal mass may also be associated with abdominal or pelvic fluid and obliteration of normal anatomical structures.¹⁰ On color Doppler, the complex adnexal mass is characterized by external vascularisation and arteriovenous shunting but without internal blood flow.¹¹ Without the use of color Doppler, 2% to 16% of ectopic gestations may be overlooked.^{12, 13}

REFERENCES

1. Bedi DG, Fagan CJ, Nocera RM. Chronic ectopic pregnancy. *J Ultrasound Med* 1984; 3: 347-352.
2. Turan C, Ugur M, Dogan M, Ekici E, Vicdan K, Gokmen O. Transvaginal sonographic findings of chronic ectopic pregnancy. *Eur J Obstet Gynecol Reprod Biol* 1996; 67: 115-119.
3. Taher MA, Sarkar AA. Ectopic gestation: utility of ultrasonography. *ASEAN J Radiol* 2002; 8: 233-234.

4. Navani H, Aggarwal BK, Chopra S Ahlawat K, Bhargava VL, Naik S. Dilemma in the diagnosis of chronic ectopic pregnancy in an unmarried girl a case report. *Asian Oceanian J Radiol* 2004; 9: 31-36.
5. Lipscomb G, Stovall T, Ling F. Nonsurgical treatment of ectopic pregnancy. *N Engl J Med* 2000; 343: 1325-1329.
6. Van Dam PA, Vanderheyden JS, Uyttenbroeck F. Application of ultrasound in the diagnosis of heterotopic pregnancy: A review of the literature. *J Clin Ultrasound* 1988; 16: 159-165.
7. Sohaye R The first trimester. In Zwiebel WJ, Sohaye R. (eds): *Introduction to Ultrasound*. 1998, Saunders, Philadelphia, pp. 372-386.
8. Maklad N, Wright MB. Grey scale ultrasound in the diagnosis of ectopic pregnancy. *Radiology* 1978; 126: 221-225.
9. Cacciatore B, Tiitinen A, Stenman U, Ylostalo P, Normal early pregnancy: serum hCG levels and vaginal ultrasonography findings. *Br J Obstet Gynaecol* 1990; 97: 899-903.
10. Rogers WF, Shanb M, Wilson R. Chronic ectopic pregnancy: ultrasonic diagnosis. *J Clin Ultrasound* 1977; 5: 257-260.
11. Abramov Y, Nadjari M, Shushan A, Prus D, Anteby SO. Doppler findings in chronic ectopic pregnancy: case report. *Ultrasound Obstet Gynecol* 1997; 9: 344-346.
12. Taylor KJW, Ramos IM, Feyock AL et al. Ectopic pregnancy: Duplex Doppler evaluation. *Radiology* 1989; 173: 93-97.
13. Atri M, Leduc C, Gillet P et al Role of endovaginal sonography in the diagnosis and management of ectopic pregnancy. *Radio Graphics* 1996; 16: 755-774.

CASE REPORT: TRAUMATIC LACERATION OF LIVER AND HAEMOPERITONIUM.

DR. MD.MURSHED ALI¹; DR. S.M.A TALEB²

A young men aged about 27 years referred for ultrasonography of the upper abdomen, having a history of blunt trauma in the right upper abdomen about ten days followed by severe upper abdominal tenderness and fever. Previously ultrasound scan was done elsewhere and the case was diagnosed as liver abscess and was treated conservatively. The condition of the patient was deteriorating day by day.

On general physical examination the patient was severely anaemic, pulse was 96 /min, Blood pressure was 110/70 mm Hg and high rise of temperature with severe tenderness in the right upper abdomen.

During ultrasound scan we found that the liver was enlarged in size, there is a large (87 mmX65mm) hypoechoic mass with irregular margin, predominantly solid in nature with peripheral hypoechoic collection in the right lobe of the liver, immediately subjacent to the diaphragm and the rest of the liver tissue was uniformly hypoechoic.

Moderate amount of free echogenic fluid collection was present in the peritoneal cavity.

The case was diagnosed as traumatic laceration of liver with haemoperitoneum. Later on, the diagnosis was confirmed by laparotomy. During laparotomy it was found that, abdominal cavity was filled-up with blood, liver, mainly the right lobe was altered in size and was lacerated. Meticulously all unhealthy liver tissue was removed and peritoneal toileting were done.

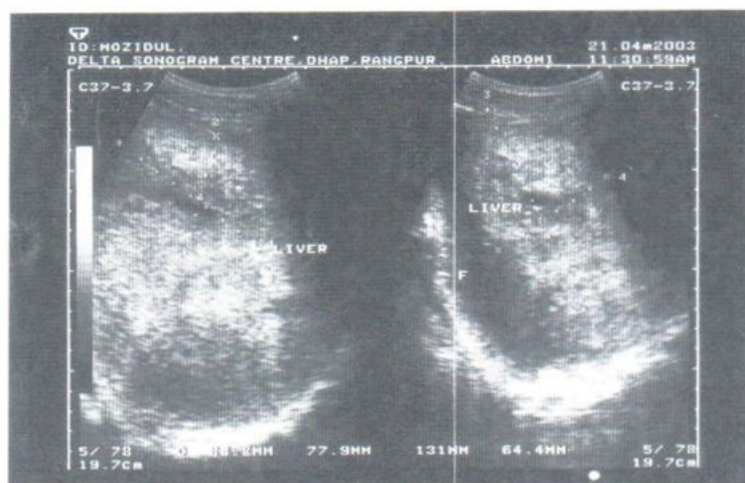


Fig.1 Sonographic Printout of Lacerated liver

1. Medical Officer, center for Nuclear Medicine and Ultrasound, Rangpur, Bangladesh.
2. Asstt. of Department of Surgery Rangpur medical College and Hospital Rangpur.

INTRODUCTION

Liver is the largest organ of the body, situated under the right hemi - diaphragm, which allow it to be protected from trauma by the costal margin. Liver is the extremely well vascularised organ and bleeding is therefore the major early complication of liver injury. The majority of injuries occurred as a result of road traffic accidents, all lower chest or upper abdominal stab wound or blunt upper abdominal trauma.

DISCUSSION

Liver trauma is a relatively rare surgical emergency but mortality and morbidity rates remain significant. It is likely that surgeons outside specialist centres will have limited experience in its management; therefore best practice should be identified and a specialist approach developed.¹

CT is the modality of reference for evaluating traumatic hepatic lesions. The selection of patients for surgery requires an accurate classification and grading of the lesions. The classification of hepatic lesions alone, however, is not sufficient, as it does not take into account peritoneal and retroperitoneal haemorrhage, which often occur, and are correlated with the need for exploratory laparotomy.

Ultrasonography can be used as a diagnostic modality where computed tomography is not

available.²

Most patients with liver trauma can be managed conservatively. Operative management carried out in non - specialized units is associated with high mortality and morbidity rates. It can be concluded that the valuable information obtained by proper ultrasound can reduce the unnecessary delay of the management, thereby relieving the patient from many morbid conditions.

Although there are different modalities for detection of liver trauma, namely USG, radioisotope scanning, CT, MRI but most agree that USG should be used as the first mean of study where CT, MRI are not easily available.

REFERECNE

1. Brammer RD, Bramhall SR, Mirza DF, Mayer AD, McMaster P, Buckels JA. In: A 10- year experience of complex liver trauma. *Br J Surg* 2002 Dec; 89(12):1532-7.
2. Miele V, Andreoli C, De Cicco ML, Buffa V, Adami EA, Regine G, Adami L, David V. In: Isolated blunt hepatic traumas: role of emergency CT in therapeutic choice. *Radiol Med (Torino)* 2002 Apr; 103 (4):360-9

CASE REPORT

DR. MD. MURSHED ALI,¹ DR. JAHARATUL FERDOUS²

CASE 1 OVARIAN PREGNANCY

Here we present a case of a 30-year-old woman with right ovarian pregnancy who came with a history of amenorrhoea for the last six months and in the early stage she had all the minor ailment of pregnancy i.e. nausea, vomiting, morning sickness etc. Previously urine for pregnancy test was done and found to be positive elsewhere with a palpable lower abdominal mobile mass. On examination, there was a mobile pelvic mass of about 17 weeks pregnancy. No foetal movement, no foetal heart sound was detected, her pulse was 88/min and blood pressure was 135/85 mm Hg and she was mild anaemic. She was diagnosed as having an ovarian tumour elsewhere and sent for ultrasonography of the pelvic organs. In ultrasonography we found that uterus is slightly enlarged in size and shape, normal in position. There is a large gestational sac with all the product of conception in it, outside the uterus, very close to the anterior abdominal wall. foetal heart movement was absent and spalding of skull bones were seen. The case was diagnosed as intra-abdominal, extrauterine pregnancy, which later on, was confirmed by laparotomy. Gestational age was calculated by femoral length of the foetus and it was about 18 weeks gestation. During laparotomy it was found that there is a large, soft mass in the pelvic cavity, clearly separated from the other intra-abdominal organs but attached to the right ovary. Within the mass we found all the foetal parts, amniotic fluid and placenta. Uterus is almost normal in size, shape and position. All the products were removed and right-sided salphingo-oophorectomy were done and the case was diagnosed finally as right-sided ovarian pregnancy.

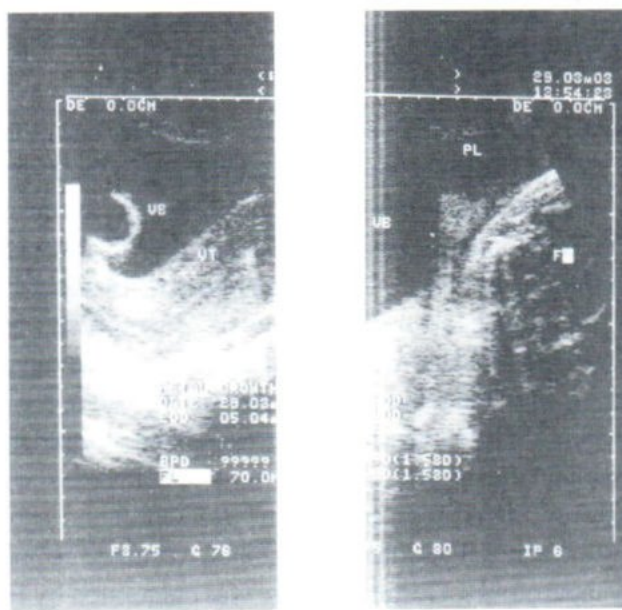
CASE 2 INTRA-ABDOMINAL PREGNANCY.

A multi-gravida aged about 33 years came with a history of amenorrhoea for 9 months without feeling of foetal movement. On general physical examination she was mild anaemic, pulse was 80/min and blood pressure was 140/80 mm Hg. Abdominal examination revealed 35 weeks size fundal height, no foetal movement and no foetal heart sound but the foetal parts were palpable very superficial near to the abdomen. Ultrasound had been done elsewhere and the case was diagnosed as intra-uterine foetal death of about 33 weeks size. Then she was hospitalized for induction of labour. The obstetrician had tried for induction of labour but failed, then she was sent for ultrasonography once more in our center. We found that the uterus was normal in size, shape, but low in position, low-placed. There is a large foetus in an amniotic cavity, outside the uterus, very close to the anterior abdominal wall. Spalding of foetal skull bones were present, foetal heart movement was absent. Amniotic fluid was almost adequate in amount and placenta was located posteriorly and maturity grade-III. The case was

¹ MBBS; M - phil (NM). Center for Nuclear Medicine and Ultrasound, Rangpur. mursedali@yahoo.com.

² MBBS; DRH (London). Head Gynae & obs. LAMB Hospital Dinajpur.

diagnosed as extra-uterine pregnancy, which later on the diagnosis was confirmed by laparotomy. During laparotomy it was found that, a dead, foetus with others product of conceptions were visualized in the amniotic cavity, outside the uterus, clearly separated from the others intra-abdominal organs and having attachment with the right ovary. All the products were removed and oophorectomy was done.



INTRODUCTION

The incidence of ectopic pregnancies has steadily increased from 4.5/1,000 in 1970 to 20/1,000 in 1992¹ prior to 1978 only 28% of ectopics were diagnosed prior to rupture; this figure had changed to be 85% by 1988^{2,3} Ectopic pregnancy is still a major cause of maternal mortality. The maternal mortality associated with an ectopic pregnancy is ten times greater than that associated with childbirth.⁴

It is more common with advancing maternal age and lower social class. History of pelvic diseases, uses of an IUCD, pelvic pain, metrorrhagia are associated with ovarian pregnancy.

DISCUSSION

Ovarian pregnancy is an uncommon type of ectopic pregnancy. Incidence has been estimated at 1 per 7 000 pregnancies and 1 to 6% of ectopic pregnancies. Pathogenesis is different from tubal

pregnancy. Generally it occurs as a single event in an otherwise healthy woman.

The most common site is the fallopian tube, although implantation can occur in the cornu, the cervix, the ovary and the abdominal cavity.⁶

Approximately 80% of ectopic pregnancies occur in the ampullary portion of the fallopian tube; 10% are in the isthmus; 5% are fimbrial in location and 2-4 % are cornual. Ovarian, cervical and abdominal pregnancies are rare.⁷

Ovarian pregnancy is a rare type of ectopic pregnancy, which is difficult to be diagnosed clinically, but its incidence is certainly underestimated.⁸

Ovarian pregnancies resulted from either ovum fertilization within the ovary (primary) or the implantation of a tubal abortion on an ovary

(secondary). The sonographic appearance of an ovarian pregnancy can vary from an "echogenic ring" fixed to the ovary to a complex adnexal mass that involves the ovary. It may, therefore, be difficult to distinguish a hemorrhagic ovarian cyst from an ovarian pregnancy.⁹

Since the fallopian tube is not affected, an ovarian pregnancy is not a risk factor for a repeated ectopic pregnancy.

An abdominal pregnancy occurs when a tubal abortion implants on a peritoneal cavity and continues to grow. While anhydramnios is common, it is not an invariable finding with abdominal pregnancies. Additional sonographic signs include a failure to visualize the uterine wall around a pregnancy; an abnormal fetal lie; and an empty uterus with an adjacent fetus. A pregnancy in one horn of a bicornuate or didelphic uterus may mimic an abdominal pregnancy.¹⁰

In most cases ovarian pregnancy mimics adnexal mass. This case was diagnosed as ovarian tumour clinically. So any adnexal mass before excision should have to use an ultrasound scanning for diagnosis.

It can be concluded that, the valuable information obtained by proper ultrasound scanning can reduce unnecessary delay in the management of many diseases, thereby relieving the patient from many morbid conditions.

Most are agreed that USG should be used as the first means of study for detection of an extra-uterine pregnancy, where TVUS facilities are not available, as it is non-invasive, hazardless and cost effective.

REFERENCES

1. NCHS: Advanced Report of final Mortality Statistics 1992 (Report No. 43, suppl). Hyattsville, MD, US Dept of Health and Human Services, Public Health Service, CDC, 1994.
2. Kim DS, chung SR, Park MI, Kim YP. Comparative review of diagnostic accuracy in tubal pregnancy: A 14-year study of 1040 cases. *Obstet Gynecol* 1987;70:547-54.
3. Stanley JH, Horger EO III, fagan CJ, Andriole JG, Fleischer AC. Sonographic findings in abdominal pregnancy. *AJR* 1986; 147:1043-1046.
4. Filly RA. Ectopic pregnancy: the role of sonography. *Radiology* 1987;162:661-668.
5. Stabile I and Grudzinskas J. In: Ectopic pregnancy: What's New?. *Progress in Obstetrics and Gynaecology*. 1994; 11: 281-310.
6. Douchar N: Nausea and vomiting in pregnancy review. *British Journal of Obstetrics and Gynaecology*. 1995;120:8-8.
7. Breen JL. A 21 year survey of 654 ectopic pregnancies. *Am J Obstet Gynecol* 1970; 106:1004-19.
8. Mathew M, AL-Hinai AM. In Primary ovarian pregnancy; *Saudi med J* 2002 Jan; 23 (1) :93-5
9. Malinger G, Achiron R, Treschan O, Zakut H. Ovarian pregnancy-ultrasonographic diagnosis. *Acta Obstet Gynecol Scand* 1988 ; 67: 561 - 563.
10. Ombelet W, Vandermerwe JV, Van Assche Fa. Advanced extra-uterine pregnancy: description of 38 cases with literature survey. *Obstet Gynecol surv* 1988;43:386 - 397.

FETAL ULTRASOUND BIOMETRY

Dr. M.A. Taher

Fetal biometry (biparietal diameter, BPD and femur length, FL) is used to establish gestational age in the first half of pregnancy and to assess fetal growth later in gestation.¹

Microcephaly is associated with many different syndromes, usually resulting in mental retardation and poor perinatal outcome.^{2,3} Microcephaly cannot be ruled out by routine second trimester ultrasound. The presence of intracranial calcification prior to 22 weeks gestation, even when the BPD is normal suggests a high risk for the development of microcephaly-serial sonograms prove helpful in the subsequent detection of head growth anomalies as in many cases microcephaly cannot be diagnosed reliably using a single screening scan in the second trimester.¹ BPD must be measured, but it is also essential to calculate the head: body ratio to exclude intrauterine growth retardation (IUGR). Isolated microcephaly, without other anomalies, is rare and the diagnosis can be difficult in borderline cases. Serial examinations at intervals of at least two weeks or even 3 weeks and very careful interpretation are necessary.⁴

A femur is short if it is more than two standard deviations (2 SD) below the mean. A skeletal dysplasia is likely only if FL is even smaller than 5 mm or smaller than 2 SD below the mean.⁴ Fetal growth is influenced by many factors e.g. race, nutrition, antenatal care, parental income etc.^{5,7}

In a fetal structural survey at 15 to 20 week's gestation, the fetuses of Asian women had less-than-expected femur lengths (-0.66 ± 1.64 mm) and the fetuses of black women had greater-than-expected femur lengths (-0.88 ± 1.57 mm) than the fetuses of white women in the second trimester.⁶ The average length of the fetal femur may even differ among

various Asian sub-populations.⁸ Parker and colleagues showed that the crown-rump length (CRL) and biparietal diameter (BPD) are similar for Asian and white fetuses up to 20 weeks.⁹ Lai and Yeo demonstrated slightly smaller BPD, head circumference, abdominal circumference and femur length (FL), more pronounced over the course of gestation in Asian compared with white fetuses.¹⁰ Fukada and colleagues showed that 7 of 549 fetuses (1.3 %) of Japanese women had femur and humerus lengths that varied more than 1.5 SD from a growth curve determined from their study population, which had no abnormalities.¹¹ Kurmanavicius et al showed almost no differences in biparietal diameter (BPD) centiles,¹² but Merz's centiles for femur length (FL) were higher than Kurmanavicius.¹³ They used a large sample size which is evenly distributed from 12 to 42 weeks of pregnancy. Raman and associates compared growth between the three different ethnic groups in the Malaysian population in a longitudinal prospective study at the University Hospital, Kuala Lumpur--the Indian fetuses had significantly longer limb lengths than the non-Indian fetuses (Malays and Chinese). Their limbs grew faster by 0.15 mm/week for femur length and 0.1 mm/week for humeral length ($P < 0.001$).¹⁴ In a study from Khulna Nuclear Medicine Centre (Bangladesh) the sensitivity of antenatal detection of intrauterine growth retardation (IUGR) by ultrasound was 76.4% with predictive value for positive test 79.2% and perinatal mortality rate 13 per thousand.¹⁵

The association between the nuchal fold and Down syndrome (trisomy 21) was first noted in

second trimester fetuses, when a nuchal thickening of 6mm or more was considered abnormal and highly predictive of Down syndrome.¹⁶ Transvaginal sonography can identify many first trimester fetuses with nuchal thickening.¹⁷ The normal first trimester fetus has an area of posterior nuchal lucency measuring less than 3 mm in thickness (anteroposterior).¹⁸ Bromley et al. Reports that fetal nose bone length is a marker for Down syndrome in the second trimester in a high-risk population.¹⁹ Yeo and coworkers state that most aneuploid fetuses have sonographically small ears ($< / = 10^{\text{th}}$ percentile for gestational age) and this smallness is not entirely related to overall small fetal size, but in almost half of the cases, the fetal ear length is disproportionately smaller than the BPD.²⁰

Rate of fetal growth, rather than fetal weight alone, is a strong predictor of adverse neonatal outcomes. Morbidity and mortality are significantly increased among fetuses with an estimated fetal weight in the 5 th percentile or less for gestational age.²¹

REFERENCES

1. Bromley B, Benacerraf BR: Difficulties in the prenatal diagnosis of microcephaly. *J Ultrasound Med* 1995; 14: 303-5.
2. Chervenak FA, Jeanty P, Cantrine F, et al: The diagnosis of fetal microcephaly. *Am J Obstet Gynecol* 1984; 149: 512.
3. Chervenak FA, Rosenberg J, Brightman RC, et al: A prospective study of the accuracy of ultrasound in predicting fetal microcephaly. *Obstetrics Gynecol* 1987; 69: 908.
4. Palmer PES (ed): *Manual of diagnostic ultrasound*, WHO & WFUMB, 2002, Geneva.
5. Taher MA. Effect of income on fetal ultrasound biometry. *Bangladesh J Ultrasonogr* 2003; 10: 12-14.
6. Shipp T D, Bromley B, Mascola M, Benacerraf B. Variation in fetal femur length with respect of maternal race. *J Ultrasound Med* 20: 141-144, 2001.
7. Jazayeri A, Porter K B, Salazar R, Sinich T. Ultrasound measured fetal biometry: Does race alter fetal growth standard? *J Ultrasound Med* 20:S 16,2001.
8. Yeo GSH, Chan W B, Lun K C, Lai F M. Racial differences in fetal morphometry in Singapore. *Ann Acad Med Singapore* 23: 371-376, 1994.
9. Parker A J, Davies P, Newton JR. Assessment of gestational age of the Asian fetus by the sonar measurement of crown-rump length and biparietal diameter. *Br. J Obstet Gynecol* 89:836-838. 1982.
10. Lai F M, Yeo GSH. Reference charts of fetal biometry in Asians. *Singapore Med J* 36: 628-636, 1995.
11. Fukada Y, Yasumizu T, Takizawa M, Amemiya A, Hosi K. The prognosis of fetuses with a shortened femur and humerus length before 20 weeks of gestation. *Int J Gynaecol Obstet* 59: 119-122, 1997.
12. Kurmanavicius J, Wright EM, Royston P, Wisser J, Huch A, Zimmermann R; Fetal ultrasound biometry: 1 Head reference values. *Br J Obstet Gynaecol* 106/2: 126-135, 1999.
13. Kurmanavicius J, Wright EM, Royston P, Zimmermann R, Huch R, Huch A, Wisser J. Fetal ultrasound biometry: 2 Abdomen and femur length reference Values. *Br. J Obstet Gynaecol* 106/2: 136-143, 1999.
14. Raman S, Teoh T, Nagaraj S. Growth patterns of the humeral and femur length in a multiethnic population. *Int J Gynecol Obstet* 54: 143-147, 1996.
15. Miah MSR, Rahman HA, Jahan N, Paul AK, Antenatal detection of intrauterine growth retardation (IUGR) by ultrasound with postnatal follow-up. In Abdullah BJJ, Kumar G, Bux SI: *Proceedings of the 6th Congress of the Asian Federation of Societies for Ultrasound in Medicine and Biology*, Kuala Lumpur (Malaysia), October 23-26,2001.

16. Benacerraf B, Barss V, Laboda L: A sonographic sign for the detection in the second trimester of the fetus with Down's syndrome. *Am J Obstet Gynecol* 151: 1078, 1985.
17. Johnson MP, Johnson A, Holzgreve W, et al: First-trimester simple hygroma: Cause and outcome. *Am J Obstet Gynecol* 168: 156, 1993.
18. Sohaye R. The fetal head, neck and face, In Zwiebel WJ and Sohaey R. introduction to Ultrasound, Saunders, Philadelphia, 1998, pp. 395-413.
19. Bromley B, Liebermann E, Shipp TD, Benacerraf BR. Fetal nose bone length: a marker for Down syndrome in the second trimester. *J Ultrasound Med* 21: 1387-1394, 2002.
20. Yeo L, Guzman ER, Ananth CV, Walters C, Day-Salvatore D, Vintzileos AM. Prenatal detection of fetal aneuploidy by sonographic ear length. *J Ultrasound Med* 22: 565-576, 2003.
21. Smith-Bindman R, Chu PW, Ecker J, Feldstein VA, Filly RA, Bacchetti P. Adverse birth outcomes in relation to prenatal sonographic measurements of fetal size. *J Ultrasound Med* 22: 347-356, 2003.

SONOGRAPHIC MEASUREMENT OF RENAL SIZE IN NORMAL BANGLADESHI CHILDREN

Ashoke Kumar PAUL,¹ Choudhury Habibur RASULX,²
Hosne Ara RAHMAN,³ Md. Sayedur Rahman MIAH⁴

SUMMARY

To assess the renal length and volume in Bangladeshi children, we prospectively studied 217 healthy children aged between 1 to 12 years using ultrasonography. The mean kidney length was 7.23 ± 0.89 cm and mean kidney volume was 47.67 ± 15.23 cm³. No significant difference in kidney length and volume was noted between boys and girls. The length and volume of left kidney was significantly larger than the right. There was a good correlation between renal volume and variables like age, body height, body weight and body surface area. The best values were found in the correlations to body surface area.

Key Words: Renal length; Renal volume; Children; Ultrasonography.

INTRODUCTION

Sonography is now playing a significant role in the evaluation of urinary tract diseases in children. Knowledge of normal renal parameters is essential for accurate evaluation of abnormal kidneys. Sonography appears to be an accurate method for measuring renal dimensions without known magnification caused by factors of chemical and photographic nature seen by excretory urography.^{1,2} There are several western sonographic evaluations of renal dimensions in normal children,^{3,4,5} but no such studies have been undertaken in this region. The aim of this study was to determine the normal renal length and volume as correlated with age, body height, body weight and body surface area in Bangladeshi children

by ultrasonography and to establish a normal reference kidney size of children in this region of Asia.

MATERIALS AND METHODS

We performed this study at the Centre for Nuclear Medicine & Ultrasound, Khulna, Bangladesh between July 2000 to June 2001. Renal sonogram was done in 217 healthy children without apparent urinary tract disease who were referred from Pediatric Unit, Khulna Medical College Hospital, Bangladesh for abdominal sonography for symptoms unrelated to urinary tract. Age ranged from 1 to 12 years; children less than 1 year old were not included

¹ MBBS, DNM Senior Medical Officer Centre for Nuclear Medicine & Ultrasound, Khulna Bangladesh

² MBBS, FCPS Associate Professor Pediatric Unit Khulna Medical College Hospital Bangladesh

³ MBBS Medical Officer Centre for Nuclear Medicine & Ultrasound, Khulna Bangladesh

⁴ MBBS, DNM Senior Medical Officer Centre for Nuclear Medicine & Ultrasound, Khulna Bangladesh

Corresponding address: Dr. Ashoke Kumar Paul Senior Medical Officer Centre for Nuclear Medicine & Ultrasound, Khulna
G P O Box # 12, Khulna- 9000 Bangladesh
E-mail<akpaul19@yahoo.com> Telephone: 880-41-762902

because of the more rapid change in kidney size during the first year of life. Patients with abnormal sonographic findings were excluded. The variables like age, body height, body weight and body surface area were recorded at the time of the examination. The body surface area (BSA) was calculated by

$$\text{BSA (m}^2\text{)} = \frac{4 \times \text{weight (kg)} + 7}{90 + \text{weight (kg)}}$$

Sonographic evaluation was done with Siemens Sonoline SL-2 real time ultrasonogram using 3.5 MHz linear transducer. All the children were examined in a prone position without any special preparations and both longitudinal and transverse scanning were performed. Length, width and thickness of both kidneys were measured. Renal

volume was calculated by volume (cm³) = Length x width x thickness x 0.523. We attempted to find relationship between renal dimensions such as renal length and volume and variables like age, height, weight and body surface area. The results were processed and analyzed using SPSS 7.0 program.

RESULTS

The length and volume of 434 kidneys was measured in 217 healthy children ranged in age from 1 to 12 years. Of them 110 were boys and 107 were girls. The mean kidney length was 7.23 ± 0.89 cm and mean kidney volume was 47.67 ± 15.23 cm³. There was no significant difference in kidney length and volume between boys and girls. The length and volume of left kidney was larger than the right and this difference is statistically significant (Table-I).

TABLE I Measurement of renal length and volume in right and left kidney separately

Parameters	Renal length (cm) (Mean ±SD) n=217	Renal volume (cm ³) (Mean ±SD) n=217
Right kidney	7.16±0.92	46.80 ±15.07
Left kidney	7.31±0.92	48.55 ±16.17
P value	<0.001	<0.001

The mean renal length and volume in different groups of age, body height, body weight and body surface area is shown in Table-II. P values are <0.001 in all those variables. So mean renal length and volume increases with rise of age, height, weight and body surface area are highly significant.

The correlation coefficient between kidney volume and body variable is shown in Table-III. There was a positive correlation found between kidney volume and age, height, weight and BSA in the total population and in each sex. The best values were found in the correlations to body surface area.

TABLE II Renal length and volume in different groups of age, height, weight and BSA

Variable	Renal length (cm) (Mean \pm SD)	Renal volume (cm ³) (Mean \pm SD)
Age (years)		
1-3 (n=25)	5.92 \pm 0.77	27.03 \pm 12.03
4-6 (n=46)	6.74 \pm 0.52	38.69 \pm 7.89
7-9 (n=69)	7.39 \pm 0.59	49.89 \pm 9.98
10-12 (n=77)	7.82 \pm 0.70	57.76 \pm 13.83
Height (cm)		
<100 (n=54)	6.35 \pm 0.80	32.82 \pm 11.64
100-119 (n=55)	7.20 \pm 0.66	47.73 \pm 12.97
120-139 (n=97)	7.62 \pm 0.63	53.93 \pm 11.74
\leq 140 (n=11)	8.37 \pm 0.59	65.14 \pm 12.38
Weight (kg)		
\leq 10 (n=19)	5.78 \pm 0.73	23.86 \pm 9.42
11-15 (n=43)	6.68 \pm 0.63	37.70 \pm 10.29
16-20 (n=56)	7.14 \pm 0.54	45.75 \pm 8.74
21-25 (n=55)	7.58 \pm 0.60	53.75 \pm 11.44
26-30 (n=34)	8.08 \pm 0.53	60.74 \pm 11.38
>30 (n=10)	8.13 \pm 0.79	68.70 \pm 10.50
BSA (m ²)		
\leq 0.600 (n=43)	6.25 \pm 0.80	30.66 \pm 11.22
0.601-0.800 (n=75)	7.05 \pm 0.58	44.24 \pm 9.65
0.801-1.00 (n=75)	7.74 \pm 0.63	55.65 \pm 11.63
>1.00 (n=24)	8.03 \pm 0.67	63.95 \pm 12.25

TABLE III Kidney volume in children correlated to age, height, weight and BSA

Variable	r value	p value
Age (years) Vs renal volume (cm ³)		
Total population (n=217)	0.700	<0.001
Boys (n=110)	0.701	<0.001
Girls (n=107)	0.691	<0.001
Height (cm) Vs renal volume (cm ³)		
Total population (n=217)	0.648	<0.001
Boys (n=110)	0.697	<0.001
Girls (n=107)	0.587	<0.001
Weight (kg) Vs renal volume (cm ³)		
Total population (n=217)	0.727	<0.001
Boys (n=110)	0.741	<0.001
Girls (n=107)	0.700	<0.001
Body surface area (m ²) Vs renal volume (cm ³)		
Total population (n=217)	0.741	<0.001
Boys (n=110)	0.764	<0.001
Girls (n=107)	0.705	<0.001

DISCUSSION

Hodson et al, in 1962 first described the measurement of renal size in children based on excretory urography.⁶ Measurement of kidney size by ultrasonography is superior to radiological measurement and presently ultrasonography is popularly used for renal dimensions. Radiographic technique yields some variability in the apparent size of the kidney due to magnification and diuretic effects of contrast material. Sonographic measurements are not influenced by the above mentioned factors. Ultrasonography is non-invasive and relatively inexpensive when compared to radiographic method. There is no radiation exposure and therefore it can be safely used in children.

In this study we found no difference in kidney length and volume between boys and girls. This finding is in good agreement with other studies.^{7,8} Several authors found no significant difference in renal length or volume between right and left kidneys.^{3,7,9} As with other study, our results showed that the length and volume of left kidney is significantly larger than the right.¹⁰

We observed that mean renal length or volume in children increases with age, height, weight and body surface area. In our series, we found significant correlation between kidney volume and variables like age, height, weight and body surface area. This finding is consistent with other studies.^{7,10} The best values were obtained in the correlations to body surface area is in agreement with the result of other study.¹⁰

CONCLUSION

Ultrasonography is a simple and convenient method of measuring kidney size in children. This study provides sonographic measurement of normal kidney length and volume in Bangladeshi children and the

result was found to be consistent with other studies elsewhere in the world.

REFERENCES

1. Effman EL, Ablow RC, Siegel NJ. Renal Growth. *Radiol Clin North Am* 1977; 15: 3-17
2. Hernandez RJ, Roznanski AK, Kuhns LR, McCormick TL. Factors affecting the measurement of renal length. *Radiology* 1979; 130: 653-656
3. Rasmussen SN, Haase L, Kjeldsen H, Hancke S. Determination of renal volume by ultrasound scanning. *JCU* 1978; 6: 160-164
4. Jones TB, Riddik LR, Harpen MD, Dubuisson RL, Samuels D. Ultrasonographic determination of renal mass and renal volume. *J Ultrasound Med* 1983; 2: 151-154
5. Hircak H, Leito RP. Sonographic determination of renal volume. *Radiology* 1983; 148: 311-312
6. Hodson CJ, Drewe JA, Karn MN, King A. Renal size in normal children: a radiographic study during life. *Arch Dis Child* 1962; 37: 616-622
7. Han BK, Babcock DS. Sonographic measurements and appearance of normal kidneys in children. *AJR* 1985; 145: 611-616
8. Holloway H, Jones TB, Robinson AE, Harpen MD, Wiseman HJ. Sonographic determination of renal volumes in normal neonates. *Pediatr Radiol* 1983; 13: 212-214
9. Rosenbaum DM, Korngold E, Teele RL. Sonographic assessment of renal length in children. 1984; 142: 467-469
10. Haugstvedt S, Lundberg J. Kidney size in normal children measured by sonography. *Scand J Urol Nephrol* 1980; 14: 251-255

UNEQUAL TWIN : CASE REPORT

Dr. M.A. Taher

Sometimes one of the twin is smaller than the other, but it is a rare phenomenon. Recently we found a twin pregnancy in a woman of 29 years, para 3, gravida 4th who complained of discomfort due to huge abdominal swelling. Ultrasonography (USG) revealed mild degree of bilateral hydronephrosis, normal hepatobiliary system, and gravid uterus with twin live fetuses of unequal sizes : biparietal diameter (BPD) 51 mm, femur length (FL) 31 and 23 mm. By menstrual history, she is running about 21 weeks of pregnancy, which corresponds to the bigger twin, but the smaller twin corresponds to about 17 weeks of pregnancy. Both the fetal hearts are beating regularly, but the smaller one is feeble and may not survive. Amniotic fluid is excessive in amount. The patient is being followed up.



Big head



Small head

DISCUSSION

Twin gestations occur once in every 85 births. Superfetation or hypercyesis is the fertilization of two ova in the same uterus at different menstrual periods within a short interval. Upto 40% of twin pregnancies are undiagnosed prior to labor and delivery. When twins are diagnosed by ultrasound early in the first trimester, in about half of these cases, one twin will silently abort and this may or may not be accompanied by bleeding. This has been termed the vanishing

twin. The incidence of birth defects in each fetus of a twin pregnancy is twice than in singular pregnancies.¹ Monochorionic pregnancies carry the risk of placental vascular anastomoses. These, if severe, may result in conditions such as the twin-twin transfusion syndrome and be seen in cases of parabiologic twinning (acephaly-acardia). Monoamniotic twins are at risk of entanglement of the umbilical cords and vascular compromise of both fetuses.² The commonest com-

plication of monochorionicity is a 5-30% risk of developing the twin transfusion syndrome (TTS).³ Unbalanced shunting of blood through placental vascular anastomoses can induce growth retardation and anemia in the donor twin while causing hydrops and polycythemia in the recipient twin.⁴ A severe form of this syndrome is the so-called 'stuck-twin' phenomenon, which occurs when the donor twin develops severe oligohydramnios and growth retardation and becomes trapped against the uterine wall by the small amniotic sac encasing it. The rarest complication in TTS is an acardiac twin (1 in 35000 deliveries). Pregnancy-related causes of polyhydramnios include congenital infections and the twin-twin transfusion syndrome (TTS). Cytomegalovirus, toxoplasmosis, listeriosis and congenital hepatitis are a few of the viral diseases that may infect a pregnancy and cause polyhydramnios.⁶ Sonographic clues that suggest infection include growth retardation and fetal cranial or liver calcifications. TTS is an uncommon entity caused by communication between the placental circulations of twins. This condition results in polyhydramnios in smaller twin. Heart failure and pericardial effusion may be present in the donor twin with TTS. A donor twin died five days after Doppler examination despite reduction amniocentesis of the polyhydramnios twin.⁷ The umbilical cord in the compromised twin showed reversal of diastolic flow. Twin reversed arterial perfusion sequence is a rare malformation with an incidence of 1 in 50000 pregnancies and results from a monochorionic twin pregnancy in which one twin has a severe abnormality involving the head and upper part of the body with a rudimentary heart. It is also caused by placental anastomotic connections leading to reversal of blood flow to one twin. Maternal indomethacin therapy may control the polyhydramnios and periodic monitoring of the pregnancy by USG should be done until delivery.⁸ The growth of one twin may serve as a marker for the growth of the other-BPD of the twins should be within 5 mm or 5% of each other and any discrepancy should not increase by greater than 3 mm over a two week period-only 77% of

growth-retarded fetuses was detected using these criteria in 1981.⁹ Using the interval growth of the femurs (FL) might be of greater value.¹⁰

REFERENCES

1. Taher's Cyclopedic Medical Dictionary 17th ed. Thomas CL, Jaypee Brothers, New Delhi, 1993.
2. Nyberg DA, Filly RA, Golbus MS, Stephens JD. Entangled umbilical Cords : A sign of monoamniotic twins. JUM 1984 ; 3 : 29-32.
3. Harrison SD, Cyr DR, Patten RM, Mack LA. Twin growth problems : causes and sonographic analysis. Semin US, CT, MRI 1993, 14(1) ; 56-67.
4. Brown DL, Benson CB, Driscoll SG et al. Twin-twin transfusion syndrome : sonographic findings. Radiology 1989 ; 170 ; 61-3.
5. Sohaey R. Amniotic fluid and fetal well-being. In Zwiebel WJ, Sohaey R : Introduction to Ultrasound, Philadelphia, WB Saunders, 1998, pp. 359-371.
6. Hill LM : Abnormalities of amniotic fluid. In Nyberg DA, Mahony BS, Pretorius DH(eds.) : Diagnostic Ultrasound of Fetal Anomalies : Text and Atlas, St Louis, CV Mosby, 1990, pp. 38-66.
7. Sohaey R, Zwiebel W. The fetal heart : A practical sonographic approach. Semin Ultrasound CT MRI 1996 ; 17 : 15-33.
8. Suresh S, Suresh I, Ganesan S. Fetal therapy. In Malhotra N (eds.) : Ultrasound in Obstetrics and Gynecology. 3rd ed. New Delhi, 2001, pp. 174-183.
9. Houlton MCC, Marivate M, Philpott RH. The prediction of fetal growth retardation in twin pregnancy. Br J Obstet Gynecol 1981 ; 88 : 264.
10. Kurtz AB, Needleman L. Ultrasound assessment of fetal age. In Callen PW : Ultrasonography in Obstetrics and Gynecology. 2nd eds. Philadelphia, WB Saunders, 1988, pp.47-64.

FUTURE OF EMERGENCY ULTRASOUND

Dr. M.A. Taher

ABSTRACT

Since 1953, abdominal ultrasound is used in the investigation and treatment of various diseases.¹ We plan to increase the use of ultrasound in emergency medicine in a cost-effective manner. In September 1979, Emergency Medicine was formally recognized as the 23rd discipline to receive specialty recognition by the American Board of Medical Specialties. About 25% of all imaging studies in the world is ultrasound examination as noted by Harvey, Pilcher and colleagues in 2002. In 1995, Wagner, Heller and Jehle recommended emergency ultrasonography in (1) acute gallbladder disease, (2) ectopic gestation, (3) obstructive uropathy, (4) abdominal aortic aneurysm, (5) traumatic hemoperitoneum, (6) pericardial tamponade. We like to add a few more: acute pancreatitis, liver abscess, molar pregnancy (gestational trophoblastic disease), acute appendicitis, twisted ovarian tumor, testicular torsion and gastric outlet obstruction.²⁻⁴

KEY WORDS: Emergency ultrasound, imaging.

INTRODUCTION

The rigid arm of the contact B-mode ultrasonography machine first available in the late 1960s, which provided bistable B-scan images was of limited usefulness for the speed required for use in emergency evaluations. By 1981, typical examinations once taking, for example, 45 minutes by a static scanner to denote, for example, a traumatic perisplenic hematoma or an intraabdominal abscess were replaced by real-time examinations that could evaluate areas of concern within minutes. Transducers could be moved rapidly from a subdiaphragmatic anterior approach to a coronal longitudinal approach through the patient's side without the necessity using a static scanner to unscrew and then screw in an appropriate transducer of push and move the machinery for the rigid transducing arm to allow it to be set up to image the patient from a different plane. Before the availability of real-time imaging, ultrasono-

graphy was truly more physically laborious. With real-time technology, findings that vary with physiologic states (eg, inspiration/expiration) could be better assessed. The basic analysis for deep venous thrombosis (ie, compressibility of a vein) could be performed. Transvaginal and transesophageal transducers were introduced in the mid to late 1980s, allowing real-time imaging of the gynecologic tract and the heart and thoracic aorta respectively, from a different vantage point (window) and using higher frequency transducers with better nearfield resolution for those examinations. Ectopic pregnancies and aortic dissections, could be better imaged. By the 1990s, new hardware and software improvements increased diagnostic capabilities. Cine loop features allowed review and retrieval of key diagnostic images obtained before the frozen image. This was particularly helpful in assessing uncooperative or uncontrollable patients,

including moving children. Duplex Doppler ultrasonography was replaced by color Doppler ultrasonography, allowing rapid visual assessment of vascular flows.

EVALUATION OF TRAUMA

Ultrasound provides potential immediate diagnosis and has capability for evaluating a multitude of injuries normally requiring several different imaging technologies e.g. foreign bodies and fractures resulting from gunshot wounds to the extremities. In the aftermath of the Armenian earthquake in 1988, sonography was used effectively as a primary screening procedure at the entry to a hospital in mass casualty patients with trauma. Only an average of 4 minutes was required to study each patient. The false-negative rate was only 1% and there were no false-positive results for trauma-associated injury of the abdomen and retroperitoneal space. On sonography, the cortex of bone is shown as a homogeneous, strong, bright reflection of echoes with deep acoustic shadowing. However, depending on the surface of the bone and the obliquity of the ultrasound beam, reverberation artifacts may also be shown deep to the cortex of the bone. With the use of a linear transducer to image the lung pleura through the anterior chest, it has been consistently found that the identification of pleural edges sliding in a to-and-fro movement with respiration definitively excludes pneumothorax. Power Doppler imaging can be used to increase the accuracy of sonography in ruling out pneumothorax. With Power Doppler imaging, the movement of the two adjacent pleural surfaces is highlighted, indicating no pneumothorax. This technique is referred to as the "power slide". Ultrasound reveals pneumothorax that is not detectable on chest X-ray and sonography is used in evaluating blunt trauma as part of the FAST (focused abdominal sonography for trauma) exam.

Indications for trauma ultrasound include blunt or penetrating trauma to the torso where there is suspicion of intraperitoneal hemorrhage, pericardial

tamponade, and hemothorax. The minimum 4 views trauma ultrasound should include the right flank to visualize the hepatorenal space, left flank to include the perisplenic anatomy, subcostal to visualize the pericardium, and pelvis to visualize retrovesical or retrouterine fluid views. The flank views also visualize the spaces above and below the diaphragm. Other views include the bilateral paracolic gutters, the apical and parasternal views of the heart, and Trendelenburg positioning with the flank views. These views assume the trauma patient is in supine position in spinal protocol with multiple other procedures required or taking place simultaneously. Limitations of trauma ultrasound include the inability to identify injury to specific viscera (contained lacerations/contusions of the spleen/liver), bowel, or retroperitoneal structures and hemorrhage. Additionally pathologic air or patient anatomy may make the examination technically difficult, and require alternative imaging modalities.

EMERGENCY ULTRASOUND IN PREGNANCY

The incidence of ectopic pregnancy has been rising over the past several decades.⁶ Most current algorithms for the evaluation of the ectopic pregnancy include the use of pelvic ultrasound with quantitative human chorionic gonadotropin (hCG) as needed. With the need to incorporate ultrasound into the standard evaluation of the symptomatic first-trimester patient with bleeding or pain, pelvic ultrasound for intrauterine pregnancy has become a natural application in emergency ultrasound. Although the number of ectopic pregnancies has increased, the mortality from ectopic pregnancies has decreased 90% since 1979. In 1978, Maklad and Wright⁷ wrote the first report of B-mode gray scale ultrasonography for ectopic pregnancy evaluation. Cacciatore et al⁸ found that a gestational sac was always seen by the time the β -hCG level reached 1000 IU (Second International Preparation Standard), and a yolk sac should always be seen by the time the mean sac diameter (MSD) reaches 10 mm (many authorities use 8 mm as the

current cutoff) on transvaginal ultrasonography.

Second and third-trimester ultrasound by emergency physicians is focused on the detection of fetal cardiac movement and the evaluation of the pregnant traumatic patient. The ultrasound is used for detection of fetal heart rate and hydrocephalus. Limitations include nonvisualization of the fetus by anatomic abnormalities or lack of heartbeat in a fetal demise. The technique for trauma ultrasound evaluation of the pregnant patient is not altered from standard techniques.

HEPATOBIILIARY SYSTEM

Cholecystitis, Cholelithiasis, pancreatitis, biliary ascariasis, peptic ulcer, and liver abscess are common differential diagnoses for pain in the epigastrium are best imaged with ultrasound. Time in the department for such patients can be saved with emergency ultrasound. Indications for biliary ultrasound include the suspicion of a biliary etiology for epigastric, abdominal, flank, or right shoulder pain. The gallbladder is visualized to detect echogenic material that may produce shadowing, gallbladder wall diameter, and presence of fluid around the gallbladder. The abnormal size of the common bile duct and the presence of a sonographic Murphy's sign should also be noted. This procedure may be performed separately or as a view of the upper abdomen in combination with other indications noted. Limitations include contracted gallbladder, nonvisualization because of bowel gas, difficulty in imaging common bile duct stones, and other pathology in the local right upper quadrant anatomy (liver, lung, or ribs).

RENAL SYSTEM

The symptoms of renal tract obstruction can require risky long or costly imaging procedures. Ultrasound of the kidneys may judge the degree of obstruction. Use of renal tract sonography can be a sensitive bedside test for hydronephrosis. Indications for the ultrasound of the renal tract include the

detection of hydronephrosis manifested by costovertebral pain, flank pain, or abdominal pain with vomiting. Both kidneys should be visualized from upper to lower pole in coronal/long and transverse planes for detection of hydronephrosis and echogenicity suggestive of stones with or without shadowing. Both kidneys can be imaged to exclude urethral obstruction. Limitations include inability to detect the cause of the obstruction or degree of renal function. Dehydration or early imaging may result in false-negative examinations, and the sensitivity of the examination is improved with hydration and serial imaging.

GASTRIC OUTLET OBSTRUCTION

Severe vomiting in a patient (infant or adult) may be investigated by ultrasound scan to look at the pylorus and adjacent region.

APPENDICITIS

Appendicitis is one of the most common acute abdominal disorders requiring emergency surgery. The misdiagnosis rate based on clinical findings is high, especially in ovulating female patients. Early real-time sonographic work was essentially limited to noting a fluid or abscess collection in cases of perforated appendicitis. We often looked for a collection on routine pelvic ultrasonography particularly near the fluid-filled bladder or anterior to the right psoas muscle. As early as 1981, A. Deutsch and G. Leopold described a case of an inflamed appendix in a patient with leukemia studied by ultrasonography. They noted the inflamed appendix as an oval mass with a "bull's-eye or targetlike" appearance. The target's central echogenicity was appendiceal mucosa, and its surrounding anechoic area represented a thickened appendiceal wall. Similar findings were discussed by Parulekar in 1983.⁹ Ooms et al¹⁰ in a review of their work using compression sonography for cases of possible acute appendicitis without a palpable appendiceal mass or evidence of perforation, showed the marked improvement in their institution's

false-negative appendectomy rates from 32% in 1985, before the report by Puylaert, 25 to 7% in 1987, through 1989, after they began performing compression sonography. Their work highlights the impact improvements in clinical ultrasonography have had on effecting true changes in patient care.

TESTICULAR TORSION

We have learned over time that torsions may be hypoechoic from edema or hyperechoic from hemorrhage. Relying on echogenicity alone for the diagnosis of testicular torsion may be problematic because the inflamed testicle of orchitis may appear hypoechoic yet may have substantial vascular flow. The key assessor of torsion is the determination of the presence or absence of intratesticular vascular flow. Whereas testicular scintigraphy was the reference standard for assessment of torsion and abnormal vascular flow to the testicle in the mid to late 1980s, by the mid 1990s, color Doppler ultrasonography had replaced it for triaging testicular torsion.

REFERENCES

1. Donald I, Mcvicar J, Brown TG: Investigation of abdominal masses by pulsed ultrasound. *Lancet* 1953;1:1188-1194
2. Harvey CJ, Plicher JM et al. Advances in ultrasound. *Clin Radiol* 2002;57:157-177
3. Wagner DK. Foreword. In Heller M, Jehle D: *Ultrasound in Emergency Medicine*. WB Saunders Co. 1995
4. Taher MA. Cost-effectiveness of abdominal ultrasonography in appendicitis. *ASEAN J Radiol* 2001; VII: 191-197 (presented in AIUM Annual convention at Orlando, Florida March 2001).
5. Cohen HL, Moore WH. History of Emergency Ultrasound. *J Ultrasound Med*. 2004; 23:451-458.
6. Lipscomb G, Stovall T, Ling F. Nonsurgical treatment of ectopic pregnancy. *N Engl J Med* 2000; 343: 1325-1329.
7. Maklad N, Wright MB. Grey scale ultrasound in the diagnosis of ectopic pregnancy. *Radio-logy* 1978; 126:221-225.
8. Cacclatore B, Tiitinen A, Stenman U, Ylostalo P. Normal early pregnancy: serum hCG levels and vaginal ultrasonography findings. *Br J Obstet Gynaecol* 1990; 97: 899-903.
9. Parulekar S. Ultrasonographic findings in disease of the appendix. *J Ultrasound Med* 1983; 2:59-64.
10. Ooms HWA, Koumans RKJ, Ho Kang Yu PJ, Puylaert JB. Ultrasound in the diagnosis of acute appendicitis. *Br J Surg* 1991; 78: 315-318.

